Applied Meteorology Unit (AMU)
Quarterly Report
First Quarter FY-98

Contract NAS10-96018

31 January 1998

Distribution:

NASA HQ/M-7/S. Oswald
NASA HQ/Q/F. Gregory
NASA HQ/M/W. Trafton
NASA HQ/AS/F. Cordova
NASA KSC/PH/R. Sieck
NASA KSC/PH/D. King
NASA KSC/PH/R. Roe
NASA KSC/AA-C/L. Shriver
NASA KSC/AA/R. Bridges
NASA KSC/MK/D. McMonagle
NASA KSC/PH-B/M. Wetmore
NASA KSC/PH-B3/T. Greer
NASA KSC/AA-C/J. Madura
NASA KSC/AA-C/F. Merceret
NASA KSC/BL/J. Zysko
NASA KSC/DE-TPO/K. Riley
NASA JSC/MA/T. Holloway
NASA JSC/ZS8/F. Brody
NASA JSC/MS4/W. Ordway
NASA JSC/MS4/R. Adams
NASA JSC/DA8/J. Bantle
NASA MSFC/EL23/D. Johnson
NASA MSFC/SA0-1/A. McCool
NASA MSFC/EL23/S. Pearson
45 WS/DOR/W. Tasso
45 WS/SY/D. Harms
45 WS/SYA/B. Boyd
45 RANS/CC/S. Liburdi
45 OG/CC/P. Benjamin
45 MXS/CC/J. Hanigan
45 LG/LGQ/R. Fore
CSR 1300/M. Maier
CSR 4140/H. Herring
45 SW/SESL/D. Berlinrut
SMC/CWP/D. Carroll
SMC/CWP/J. Rodgers
SMC/CWP/T. Knox
SMC/CWP/R. Bailey
SMC/CWP (PRC)/P. Conant
Hq AFSPC/DDOR/G. Wittman
Hq AFSPC/DRSR/S. Heckman
Hq AFMC/DOW/P. Yavosky
Hq AFWA/CC/J. Hayes
Hq AFWA/DNXT/D. Meyer
Hq AFWA/DN/L. Freeman
Hq AFWA/DNXM
Hq USAF/XOW/F. Lewis
AFCCC/CCN/M. Adams
Office of the Federal Coordinator for Meteorological Services and Supporting Research
SMC/SDEW/B. Hickel

SMC/MEEV/G. Sandall
NOAA "W/OM"/L. Uccellini
NOAA/OAR/SSMC-I/J. Golden
NOAA/ARL/J. McQueen
NOAA Office of Military Affairs/T. Adang
NWS Melbourne/B. Hagemeyer
NWS/SRHQ/H. Hassel
NWS "W/SR3"/D. Smith
NSSL/D. Forsyth
NWS/"W/OSD5"/B. Saffle
NWS/"W/OSD23"/D. Kitzmiller
PSU Department of Meteorology/G. Forbes
FSU Department of Meteorology/P. Ray
NCAR/J. Wilson
NCAR/Y. H. Kuo
30 WS/CC/C. Davenport
30 WS/DOS/S. Sambol
30 SW/XP/R. Miller
NOAA/ERL/FSL/J. McGinley
SMC/CLNM/B. Laine
Aerospace Corp./B. Lundblad
Tetratech/NUS Corp./H. Firstenberg
ENSCO ARS Div. V.P./J. Pitkethly
ENSCO Contracts/M. Penn

Executive Summary

This report summarizes AMU activities for the first quarter of FY 98 (October - December 1997). A detailed project schedule is included in the Appendix.

During this quarter, AMU personnel supported six expendable vehicle launches and one Shuttle mission at Range Weather Operations. The AMU Mid-Course Review teleconference was held on 24 November with representatives from SMG, 45 WS, KSC, NWS MLB, and the AMU. The extension of the 915 MHz profiler network data quality control task and the evaluation of the SIGMET system for the 45 WS WSR-74C radar were discussed.

Dr. Manobianco traveled to Tallahassee, FL in October for technical interchange with the Cooperative Institute for Tropical Meteorology at the Florida State University and the NWS Weather Forecast Office in Tallahassee where he presented results on the AMU's meso-eta model evaluation. He also attended the U.S. Weather Research Program Data Assimilation Workshop held in Monterey, CA in December. The purpose of the workshop was to develop a 5-year science/research plan on data assimilation with the objective of improving numerical predictions from several hours to ten days. Mr. Wheeler attended the National Weather Association 22nd Annual Meeting in Reno, NV where he presented two posters describing the results of the AMU's Radar/PIREP and 915 MHz profiler data quality control tasks. These meetings provided an opportunity to receive comments and suggestions on our work from other experts in the field and to take advantage of their experiences with similar projects.

Mr. Wheeler distributed the final memorandum describing the results of the Microburst Day Potential Index evaluation in November. He also completed the analyses of thunderstorm cell attributes and trends in hail and high wind cases for the NEXRAD Exploitation task. Mr. Wheeler's findings from these analyses are presented in this report.

Dr. Taylor and Ms. Lambert continued developing and testing 915 MHz wind profiler data quality control routines during the quarter. The best results came from a combination of a consensus time period check, a rain contamination check, and the Weber-Wuertz algorithm. A description of the quality control routines and a discussion of their results are given in this report.

Mr. Evans continued analyzing the plume resulting from the Delta 2 explosion on 17 January 1997 using WSR-88D radar observations and the atmospheric models REEDM, RAMS, and HYPACT. Preliminary results from his analyses are presented in this report. Mr. Evans also produced RAMS and HYPACT data for the MVP Session III and sent the results to NOAA/ATDD. Data are currently being produced for Sessions I and II.

Mr. Nutter continued the objective evaluation of the meso-eta model surface and upper-air point forecast accuracy. Statistics were generated for the forecasts of temperature, mixing ratio, and wind speed using the 1996 warm and cool season and 1997 warm season data sets. The preliminary results are presented in this report. Dr. Manobianco and Mr. Nutter completed data collection for a central Florida warm season case study, installed and configured a Local Data Integration System, and began investigating its utility through analysis of a warm season weather event. A description of the data, the LDIS, and a discussion of the preliminary results are given in this report.

Dr. Merceret continued to advise John Lane, a Ph.D. candidate at the University of Central Florida, on a study of raindrop size distributions and their effect on Z-R relations. The work is directed at improving the use of WSR-88D and raingauge data as ground truth for NASA's TRMM project. In November, Mr. Lane and Dr. Merceret met with Paul Willis, an expert in tropical cloud physics, at the Hurricane Research Division of NOAA/ERL in Miami to discuss the work.

SPECIAL NOTICE TO READERS

AMU Quarterly Reports are now published on the Wide World Web (WWW). The Universal Resource Locator for the AMU Home Page is:

http://technology.ksc.nasa.gov/WWWaccess/AMU/home.html

The AMU Home Page can also be accessed via links from the NASA KSC Internal Home Page alphabetical index. The AMU link is "CCAS Applied Meteorology Unit".

If anyone on the current distribution would like to be removed and instead rely on the WWW for information regarding the AMU's progress and accomplishments, please respond to Frank Merceret (407-853-8200, francis.merceret-1@ksc.nasa.gov) or Ann Yersavich (407-853-8203, anny@fl.ensco.com).

1. BACKGROUND

The AMU has been in operation since September 1991. The progress being made in each task is discussed in Section 2 with the primary AMU point of contact reflected on each task and/or subtask.

2. AMU ACCOMPLISHMENTS DURING THE PAST QUARTER

2.1 TASK 001 AMU OPERATIONS

During October Mr. Wheeler traveled to Reno, NV to attend the National Weather Association 22nd Annual Meeting where he presented two posters: 1) Final Report on the Radar/PIREP Cloud Top Discrepancy Study and 2) Data Quality Assessment Methods for the 915 MHz Profiler Network on Kennedy Space Center/Cape Canaveral Air Station. Mr. Wheeler and Mr. Bill Roeder (45 WS) met with Margot Ackley (NOAA/ETL) and Seth Gutman (NOAA/FSL) on a possible project using GPS integrated water vapor data in forecasting. A meeting was also held with Mr. Gary Ellrod (NOAA/NESDIS) on a possible project to study the use of a satellite-derived Microburst Day Potential Index computed hourly.

Dr. Manobianco and Mr. Daniel Petersen (NWS MLB) traveled to Tallahassee, FL on 27-29 October for technical interchange with the Cooperative Institute for Tropical Meteorology (CITM) at the Florida State University (FSU) and the NWS Weather Forecast Office in Tallahassee. The trip was sponsored by the NWS Southern Region Headquarters and CITM. While in Tallahassee, Dr. Manobianco presented results on the AMU's meso-eta model evaluation as part of the weekly seminar series at FSU. Dr. Manobianco and Mr. Petersen met with several members of the NWS TLH WFO to discuss NWS TLH efforts in setting up local mesoscale modeling using MM5 and developing sea breeze climatologies using satellite and rawinsonde data.

Dr. Manobianco and Mr. Petersen met with Dr. Krishnamurti at FSU and two post-doctoral students who are running 7-day ensemble forecasts of tropical cyclones under contract with a Bermuda insurance company. While at FSU, they also met with Dr. Henry Fuelberg's graduate students. Dr. Fuelberg's students, in collaboration with Mr. Bill Roeder (45 WS) through AFIT, are focusing on high resolution simulations of Florida's east coast sea breeze and thunderstorm probabilities at KSC/CCAS derived from statistical relationships between low-level convergence and stability.

The AMU Mid-Course Review teleconference was held on 24 November. Representatives from SMG, 45 WS, KSC, and NWS MLB discussed two AMU tasks for the 6 months leading to the annual tasking meeting in May 1998. The first item discussed and agreed upon was the extension of the 915 MHz profiler network data quality control (QC) to include the RASS virtual temperature data. This data type will be examined for its usefulness in forecasting certain weather phenomena and it is, therefore, important that it be QC'd prior to analysis. The second item was the AMU task to evaluate the new

SIGMET display system for the 45 WS WSR-74C radar. The AMU will evaluate products, including integrated reflectivity (lightning and microburst nowcasting) and layered reflectivity products (cloud monitoring), for their forecasting utility in support of ground and launch operations. SIGMET is a new system and issues dealing with hardware/software performance could affect the task progression. Thus, exact specifications on final products are difficult to define and must remain flexible.

Dr. Manobianco attended the U.S. Weather Research Program (WRP) Data Assimilation Workshop held in Monterey, CA from 9-11 December. The purpose of the workshop was to develop a 5-year science/research plan on data assimilation with the objective of improving numerical predictions from several hours to ten days. Dr. Manobianco was an active participant in all phases of the workshop, especially the breakout sessions on predictability of high impact weather and advanced assimilation techniques for short-term predictions. During off-line conversations with Dr. J. Arnold (NASA Program Director for USWRP) and Dr. R. Carbone (NCAR - USWRP Lead Scientist), Dr. Manobianco learned that the schedule for 1998 USWRP proposal submission will be delayed approximately two months. The first step in possible NASA (KSC)/AMU participation in the USWRP would be to submit a pre-proposal in the spring 1998. The pre-proposal would outline Dr. Merceret's plan to improve coastal mesoscale forecasting in east central Florida by leveraging existing resources such as comprehensive mesoscale data sets, local mesoscale models, and expertise in modeling and data assimilation.

Mr. Wheeler relocated several pieces of hardware and reconfigured others to make room in the AMU laboratory for the MIDDS upgrade hardware (two Hewlett Packard (HP) workstations) and the SIGMET radar processor hardware (one HP workstation). In November we removed our Wide Workstation MIDDS hardware and reconfigured the remaining OS/2 MIDDS system to handle all of our data requests and product generation for weather review. Starting in 1998 the weather display system will be rehosted onto HP UNIX platforms as a UNIX based weather data distributed system. The weather display software will be McIDAS-X.

SUBTASK 3   MICROBURST DAY POTENTIAL INDEX (MDPI) EVALUATION (MR. WHEELER)

As part of the 1997 Microburst Task, the AMU was assigned to fine tune the MDPI as a technique for forecasting the potential for damaging winds at CCAS and KSC. Results from the 1997 season (POD 97%, FAR 27%, CSI 69% and HSS .71) prove the MDPI continues to be a reliable microburst indicator. All of these results were similar to those for 1995. The final memorandum was distributed in November 1997. This task is now completed.

2.2   TASK 004   INSTRUMENTATION AND MEASUREMENT

SUBTASK 1   NEXRAD EXPLOITATION (MR. WHEELER)

During this quarter Mr. Wheeler completed entering the cell trend attribute data into a spreadsheet. The cell trend attributes include maximum reflectivity, height of the maximum reflectivity, storm top and base, hail and severe hail probabilities, cell-based VIL and core aspect ratio. He completed analyzing the trends and thresholds of each cell's attributes. The publication of the final report is behind schedule due to the reconfirmation of several cell attribute trends through WATADS, the installation of the MIDDS Upgrade and SIGMET computer equipment, and the holidays. A portion of the results to appear in the final report are presented in this section.

Archived level II radar data from the NWSFO at Melbourne, FL was used. Analysis of the radar data was done using WATADS build 9 so the algorithms matched those being used on the operational PUP. Similar to the PUP, WATADS build 9 has the capability to monitor the cell trend information on each identified storm cell. The analysis procedures were to identify each cell and track the maximum reflectivity, height of maximum reflectivity, storm top and base, hail and severe hail probabilities, cell-based VIL and the core aspect ratio using the cell trend information from WATADS.

The Storm Cell Identification and Tracking (SCIT) algorithm had a difficult time with small cells associated with typical Florida weather regimes. During the analysis, there were numerous occasions when the tracking of a cell would be lost or a new cell would be identified in the same location as the cell being tracked.

For the wind and hail cases, trends were noted in height of maximum reflectivity and cell-based VIL. Prior to the reported hail events, the height of the maximum reflectivity increased by 4000 ft or greater and the cell-based VIL increased by 10 kg/m^2 or more during one 5-minute volume scan period. Figure 1 details the change in height of the maximum reflectivity and the cell-based VIL. Notice the rapid increase in these parameters between 1432 and 1437 UTC in Fig. 1. The height of the maximum reflectivity increased from 14000 to 27000 ft and the cell-based VIL increased from 33 to 45 kg/m^2. Hail was reported in the Orlando area (Forest City) at 1450 UTC.

Cell 47, Near Orlando
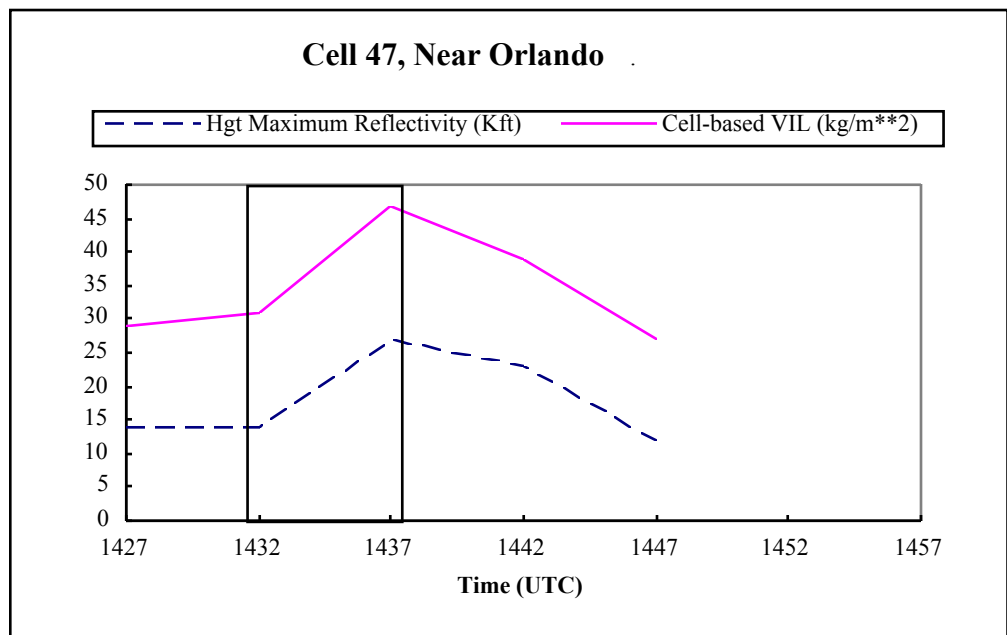
Figure 1.   Height of maximum reflectivity and cell-based VIL plotted versus time for storm cell which reported hail on 23 April 1997 (box highlights change period).

For significant wind events (i.e. reported wind damage and/or winds >35 kt on the KSC/CCAS wind towers), a decreasing trend in the height of maximum reflectivity and cell-based VIL was noted. The height of the maximum reflectivity decreased by 4000 ft or greater and the cell-based VIL decreased by 10 kg/m^2 or greater during one 5-minute volume scan. Figure 2 illustrates trends in the height of maximum reflectivity and cell-based VIL for a cell that was in the CCAS area on 11 July 1995. A microburst was reported at 1910 UTC as this cell moved through the CCAS area. Note the rapid decrease in the height of the maximum reflectivity from 24000 to 10000 ft and the cell-based VIL from 32 to 12 kg/m^2 between 1847 and 1852 UTC (i.e. box in Fig. 2).

For non-significant storm cells (i.e. those not associated with hail or wind damage), trends in **both** the height of the maximum reflectivity and the cell-based VIL did not follow patterns similar to those for significant events. An example of trends for these variables from a non-significant storm cell observed on 29 March 1997 is shown in Figure 3. In this particular example, the increase in the cell-based VIL does not meet the 10 kg/m^2 threshold change criteria.

In summary, two case days were analyzed during the warm (June - September) and cool season (January - April) for a total of four case study days. In the data that were analyzed, the height of

maximum reflectivity and cell-based VIL showed a signature prior to both hail and significant wind events. The trends give the radar operator a 5 to 15-minute warning prior to these weather events. The WSR-88D SCIT algorithm does have difficulty in keeping track of cells in the central Florida area. The WSR-88D Cell Trend final report will be completed and distributed in early February 1998.

Cell 76, CCAS

- - - Hgt Maximum Reflectivity (Kft) ——— Cell-based VIL (kg/m**2)
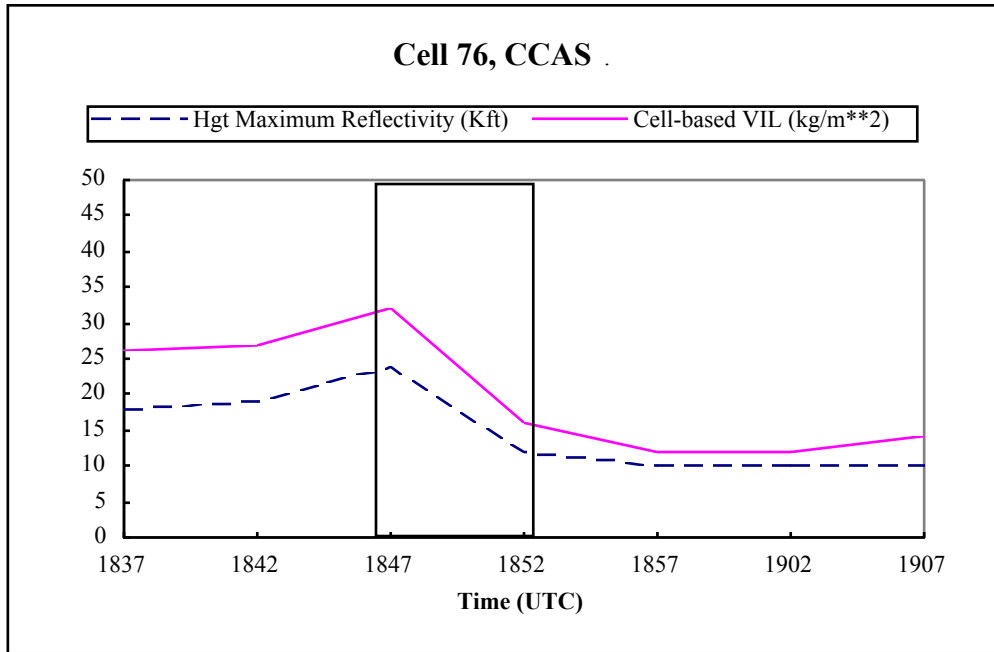
Figure 2.   Height of maximum reflectivity and cell-based VIL plotted versus time for a microburst event at CCAS on 11 July 1995 (box highlights change period).
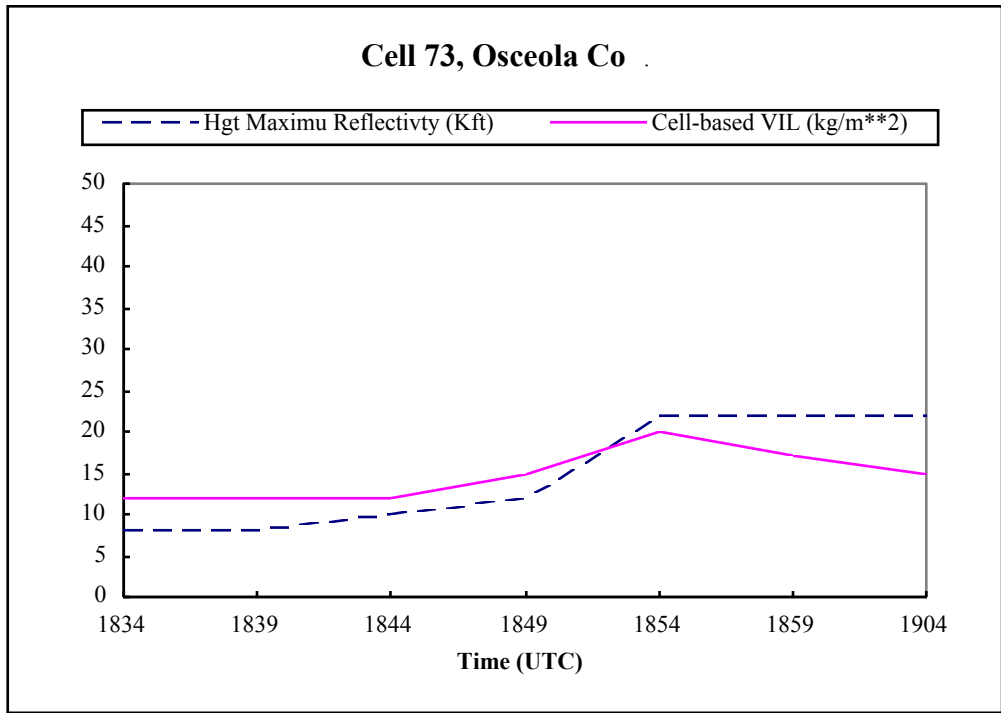
Figure 3. Height of maximum reflectivity and cell-based VIL plotted versus time for a typical non-event storm cell on 29 March 1997.

SUBTASK 2   915 MHZ BOUNDARY LAYER PROFILERS (DR. TAYLOR)

In October, Dr. Taylor and Ms. Lambert attended a working group meeting to discuss the RSA proposal to relocate the False Cape profiler. Ms. Lambert discussed the meteorological concerns to be addressed and presented the results of the calculations showing the effect the new network configuration would have on the area-averaged divergence (AAD) calculations. Mr. Mike Maier of CSR wrote a draft document outlining the concerns of the working group. Dr. Taylor and Ms. Lambert provided comments on the document before it was sent to the appropriate personnel in RSA.

Dr. Taylor and Ms. Lambert continued developing and testing data QC routines during the quarter. They included large and small median tests, a signal-to-noise ratio check, a rain contamination check, a consensus time period check, and the Weber-Wuertz algorithm (WW; Weber and Wuertz 1991). The best results came from a combination of the consensus time period check, the rain contamination check, and WW.

These algorithms were analyzed by using the color displays of wind speed and direction described in previous reports. These color displays highlight the areas of bad data and facilitate analysis of the effectiveness of the QC routines used. The raw data values were used to verify whether suspect data were actually erroneous and to determine input parameters to each of the QC routines. A description of the QC algorithms and their results are given below. A description of the profiler network can be found in the AMU Quarterly Report Fourth Quarter FY-97.

The QC Algorithms

Three QC algorithms are applied to the data. The consensus time period algorithm checks the number of minutes in the consensus period. Wind data calculated from periods of less than 6 minutes are flagged as suspect. The rain contamination algorithm determines if rain is detected by the vertical beam and flags the corresponding horizontal winds. The WW is a pattern recognition program that is

9

well known and widely used in the profiler community. If a datum or data pattern does not meet the pattern recognition criteria in the program, it is flagged.

Consensus Time Period Check

This algorithm was made necessary by a system check that will reset a profiler if its computer time is more than 5 seconds off the central computer time (located in the ROCC). When it is reset during a consensus period all data collected up to the time of the reset is erased, but the profiler will continue to collect data through the end of the allotted period and calculate a consensus wind. If the reset occurs toward the end of the period, a consensus wind is calculated from data collected over a very short time period. This tends to create erroneous wind profiles.

This reset procedure rarely occurs, but because it does occur and create erroneous profiles, the time periods must be checked. If a profile is calculated from a consensus period of less than 6 minutes, it is flagged as suspect.

Rain Contamination Check

Ralph et al. (1996) show that rain can contaminate 915 MHz profiler data and will be seen as strong downward vertical velocities in the vertical beam. Strong downward velocities and high SNRs in the data sets were often associated with erroneous profiles when rain was reported over the Cape area. Plots of SNR versus. vertical velocity revealed two distinct populations separating clear-air and rain contaminated data points. This allowed development of the discriminant function (Panofsky and Brier 1968)

$$L = -1.731 + 0.298(VV) + 0.014(SNR)$$

where VV is the vertical velocity in knots and SNR is in dB. If the result, L, is positive, the data point is considered to be contaminated by rain and is flagged as suspect.

Weber-Wuertz Algorithm

The Weber-Wuertz algorithm (WW) will recognize patterns in one- or two-dimensional arrays of any desired data type. It is currently set up to recognize patterns in time and space in the individual consensus radial velocities of the three beams used in the consensus. WW requires that certain parameters be set that dictate how the program will establish patterns. Several iterations of tests were done using several data sets to determine the appropriate settings. The parameters and their settings are shown in Table 1.

Table 1.	Weber-Wuertz Algorithm Parameter Settings.
Parameter	*Value*
dx: time space (along radial)	30 minutes (2 time periods) 631.4 feet (194 m or 2 gates)
dy: oblique beams vertical beam	4 knots 2 knots
nmin	32 data points

WW defines dx as the neighborhood size in both time and space as noted in Table 1. dy is defined as the acceptable change in wind speed over the neighborhood size. In other words, dy/dx can be viewed

as the maximum allowable derivative for continuous data in a pattern. The minimum number of data points any pattern can have is defined by nmin. Patterns with less than 32 data points are considered unreliable and are flagged as suspect by the algorithm.

Order of Algorithms

The algorithms must be used in a certain order. The consensus time period and rain contamination checks do not depend on time or space continuity of the data and are run first to remove the obviously bad data. This is to ensure that WW will not see areas of bad data as legitimate patterns. When run in this order, the algorithms do very well in flagging most of the bad data points while flagging very few good data points.

Results

The results of the data QC using the three routines are shown using data from the False Cape profiler (see Fig. 4) collected on 17 June 1997. Color displays of wind speed and direction are used to help locate the obvious areas of erroneous data.

On 17 June, thunder showers were reported over the KSC/CCAS area beginning at 1630 UTC and extending to 2200 UTC, the same period over which most of the erroneous profiles were seen. Figures 4 and 5 show the wind speed and direction, respectively, from 17 June before the data QC. The black areas show the levels at which a consensus was not reached. The bad data can be identified by inconsistencies in time and space of both the wind speed and direction. Most notable are the inconsistencies found between 1700 - 1800 UTC from approximately 5000' - 10000', between 1930 - 2000 UTC through the entire profile, between 2030 - 2100 UTC from 7000' - 10000', and at 2130 from 3000' - 7000'.

Figures 6 and 7 show the wind speed and direction, respectively, after the data QC. The black areas show the levels where data were flagged as bad in addition to those levels where a consensus was not reached. Most of the bad data have been removed, but some questionable data still remain in the two profiles at 2000 and 2015 UTC.

17 JUNE 1997 WIND SPEED
False Cape Profiler
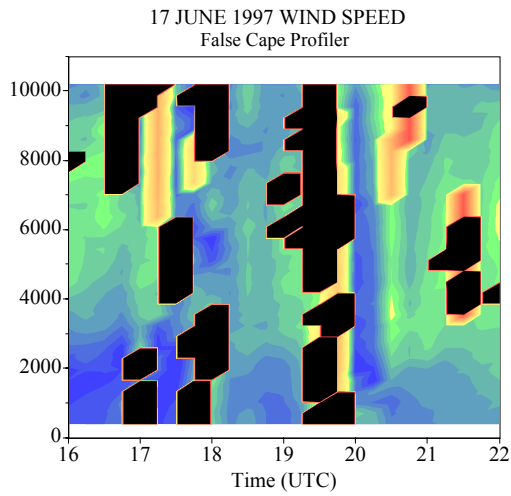
Figure 4.　17 June 1997 False Cape profiler display of wind speed from 1600 to 2200 UTC before data QC. Heights are in feet and wind speeds are in knots.

17 JUNE 1997 WIND DIRECTION
False Cape Profiler
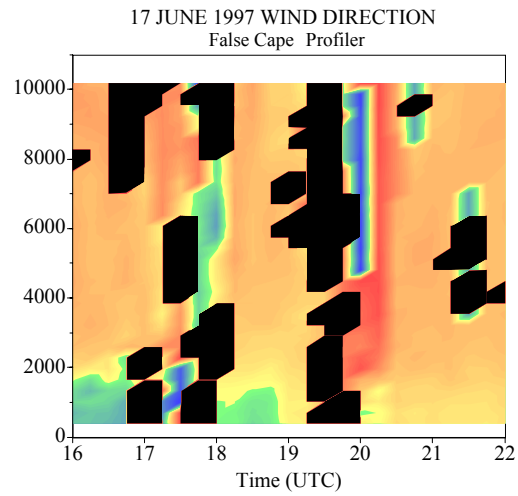
Figure 5.　17 June 1997 False Cape profiler display of wind direction from 1600 to 2200 UTC before data QC. Heights are in feet and wind directions are in degrees.

17 JUNE 1997 WIND SPEED
False Cape Profiler
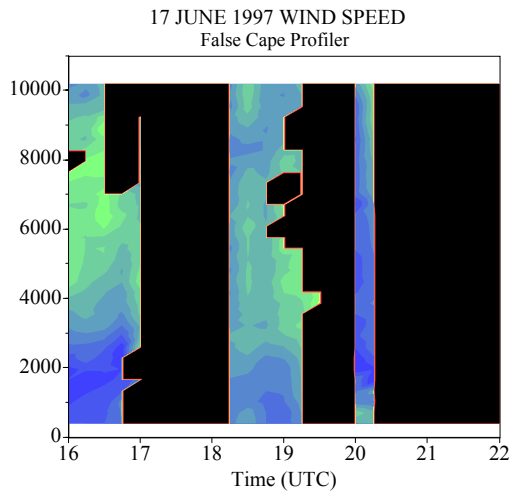
Figure 6.　17 June 1997 False Cape profiler display of wind speed from 1600 to 2200 UTC after the data QC. Heights are in feet and wind speeds are in knots.

17 JUNE 1997 WIND DIRECTION
False Cape Profiler
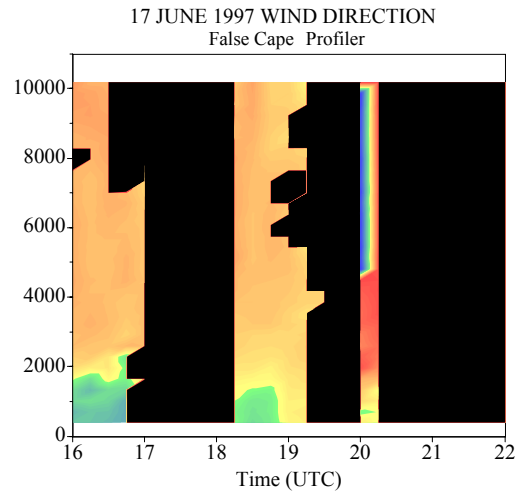
Figure 7.　17 June 1997 False Cape profiler display of wind direction from 1600 to 2200 UTC after data QC. Heights are in feet and wind directions are in degrees.

12

Summary

The results show that the consensus time period check, rain contamination check, and WW are effective in flagging most of the erroneous consensus wind data. The order in which the algorithms are run is important. The consensus time period and rain contamination checks are run first to remove obviously bad data points. Weber-Wuertz will then not see large areas of bad data as good patterns.

References

Heckman, S. T., M. W. Maier, W. P. Roeder, J. B. Lorens, and B. F. Boyd, 1996: The operational use of a boundary layer profiler network at the Eastern Range and Kennedy Space Center, *27th Conference on Radar Meteorology*, Vail, CO, 346-348.

Panofsky, H. A., G. W. Brier, 1968: *Some Applications of Statistics to Meteorology.* The Pennsylvania State University, 224 pp.

Ralph, F. M., P. J. Neiman, D. Ruffieux, 1996: Precipitation identification from radar wind profiler spectral moment data: vertical velocity histograms, velocity variance, and signal power - vertical velocity correlations. *J. Atmos. Oceanic Technol.*, **13**, 545-559.

Weber, B.L. and D. B. Wuertz, 1991: Quality control algorithm for profiler measurements of winds and temperatures. NOAA Tech. Memo. ERL WPL-212, 32pp.

SUBTASK 5   I&M AND RSA SUPPORT (DR. MANOBIANCO/MR. WHEELER)

Mr. Wheeler supported several meetings and the factory acceptance testing for the Advanced MIDDS during November. In early November, Mr. Wheeler visited PRC Inc.'s Virginia office as a member of the 45 WS support team to view PRC's demonstration of the functionality of the Advanced MIDDS. Several shortfalls were documented and passed on to the 45 Space Program Office (SPO) and PRC. The team was also shown WFO-Advanced Forecast System (NWS weather display system). As a result of this visit, it was determined that the current configuration of Advance MIDDS would not met the functionality or requirements for the 45 WS.

After the acceptance testing, Mr. Wheeler supported several meetings with the 45 WS and one with the 45 SPO on options available for the 45 WS to implement a new weather display system. It was determined that McIDAS-X is the best solution as the display software on the new HP platforms. Mr. Bolton (of CSR Weather) developed a 3-phase approach to installing McIDAS-X as a stand-alone weather display system that will occur over a 2-9 month period. In the first 6 weeks, several display terminals would be setup as McIDAS-X display systems but at the end of that period the current main-frame system would be removed.

2.3   TASK 005   MESOSCALE MODELING

SUBTASK 4   DELTA EXPLOSION ANALYSIS (MR. EVANS)

The Delta Explosion Analysis project is being funded by KSC under AMU option hours. The primary goal of this task is to conduct a case study of the explosion plume using the RAMS and REEDM models and compare the model results with available meteorological and plume observations. The RAMS model was run using both ERDAS and PROWESS. ERDAS contains version 3a of RAMS which is configured to run with 3 nested grids, inactive microphysics, and a fine grid spacing of 3 km. PROWESS contains version 4a of RAMS which is configured to run with 4 nested grids, active microphysics, and a fine grid spacing of 1.5 km.

The rocket exploded 12.5 seconds after liftoff at a height of approximately 484 meters. This initial explosion destroyed only the first stage and the boosters and produced a large cloud extending from the ground upward. The Delta 2 is a three-stage liquid-propellant vehicle with nine solid-propellant strap-on booster motors. The second and third stages and payload survived the initial explosion and continued upward to about 760 meters at 22.4 seconds. Destruct signals were sent at this point, and the exploding second-stage formed a buoyant cloud that rose above and separated from the lower cloud. Figure 8 shows a frame extracted from a video which was taken by a viewer located in Cape Canaveral, south of CCAS. The picture clearly shows the two clouds produced from the explosion of the vehicle.

The Melbourne WSR-88D radar data was preliminarily analyzed and provided information on the track of the clouds following the explosion. The radar is located approximately 37 km south of Cape Canaveral and scans a horizontal radial of 360 degrees at five vertical elevation angles ranging from 0.5 to 4.5 degrees every 10 minutes.

Radar reflectivity measurements of the resulting cloud provided good estimates of the location and dimensions of the cloud over a 4-h period after the explosion. Figure 9 shows the plume height of the lower cloud (Plume 1) and Fig. 10 shows the plume height of the upper cloud (Plume 2) over the 4-h period. The data were obtained by subjectively analyzing the archived radar data.

The lower cloud height data indicate that Plume 1, which moved south over the Melbourne area, initially reached up to a height of approximately 2.7 km. From 30 minutes after the explosion until 4 hours afterward, the lower cloud height remained below 1.5 km. The radar data indicated that the lower limit of the cloud reached no lower than 40 m above the ground at approximately 60 minutes after the explosion. The upper cloud height data indicate that Plume 2, which moved east out over the ocean, reached as high as 4.5 km but never went below 0.5 km. The radar data are being compared to model output produced by HYPACT simulations that were initialized with data from the PROWESS version of RAMS and data from the ERDAS version of RAMS.

All data presented in this report are preliminary and are still undergoing analysis. Model analysis and data reduction will continue on this task and all results will be included in the final report expected to be distributed in March 1998.
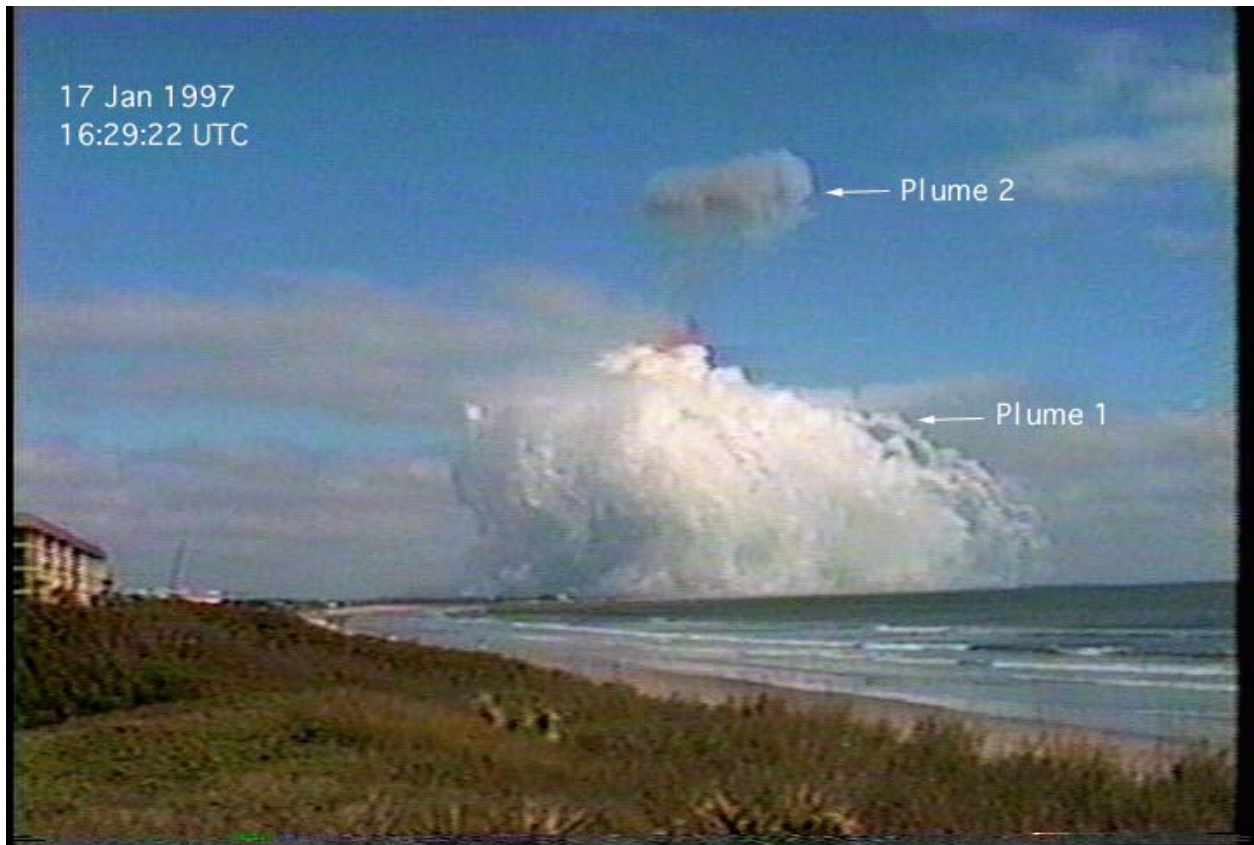
Figure 8.   The two clouds produced from the explosion of the vehicle.
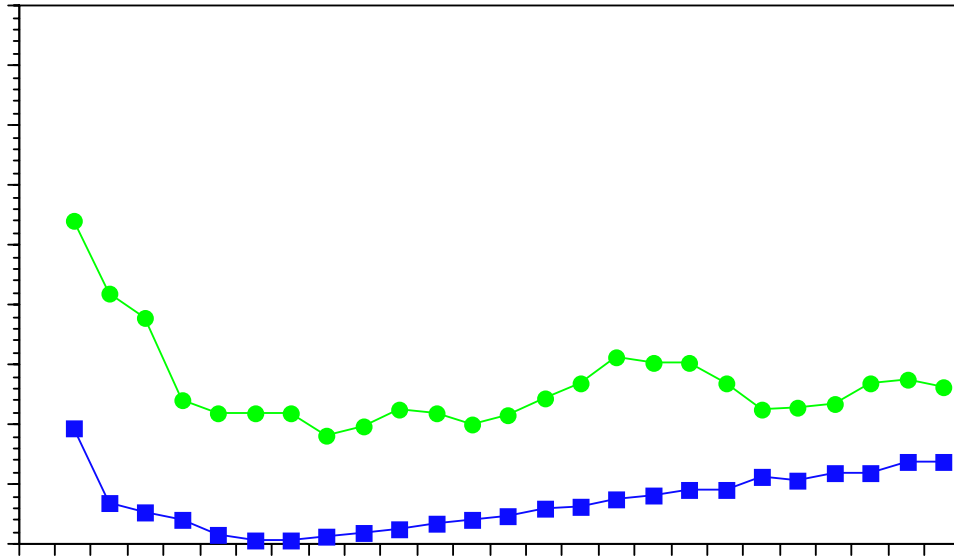
Figure 9.   The plume height of the lower cloud (Plume 1) over the 4-h period.
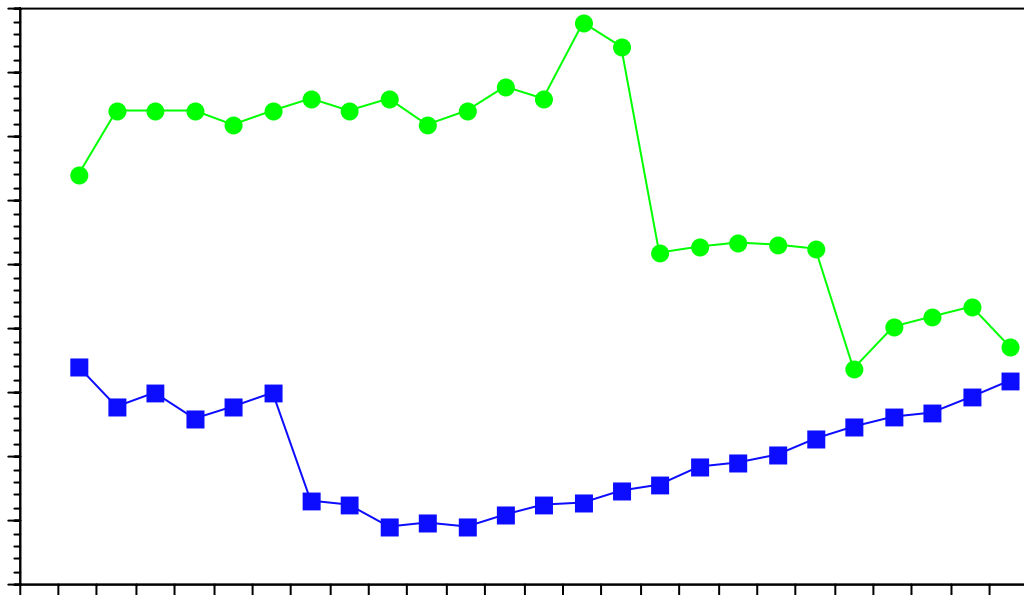
Figure 10.   The plume height of the upper cloud (Plume 2) over the 4-h period.

SUBTASK 5   MODEL VALIDATION PROGRAM (MR. EVANS)

The primary purpose of the U.S. Air Force's Model Validation Program (MVP) Data Analysis project, which is being funded by option hours from the U.S. Air Force, is to produce RAMS and HYPACT data for the three MVP sessions conducted at Cape Canaveral in 1995-1996. This program involves evaluation of Range Safety's modeling capability using controlled releases of tracers from both ground and aerial sources.

Thus far we have:

- Configured HYPACT to run on the PROWESS workstations and

- Determined the source configuration to be used for HYPACT input.

Several different HYPACT configurations were tested for the MVP Session III data to determine the best configuration with respect to the source term to represent the MVP releases. The configuration options are number of particles, source length, width and height, source duration, and grid spacing. A SAS software routine was developed to analyze and display the GPS blimp locations and was used to help determine some of the input source characteristics. We also modified HYPACT to get the output to conform to the desired format.

- Once the source configuration was finalized, the HYPACT simulations for all of the continuous plume releases for Session III were made.

- The Session III RAMS and HYPACT data has been sent to NOAA/ATDD for their model evaluation analyses. The data were sent on four 4-mm tapes. Tape contents are:

  - tape1: PROWESS RAMS data from 29 April 1995 -2 May 1995 (approx. 2 Gigabytes)

  - tape2: PROWESS RAMS data from 3 May 1995 - 9 May 1995 (approx. 1.5 Gigabytes)

  - tape3: ERDAS RAMS data from 29 April 1995 - 9 May 1995 (approx. 1.3 Gigabytes)

  - tape4: HYPACT data for each MVP III release generated from PROWESS and ERDAS RAMS data (approx. 1.3 Gigabytes)

A listing of the HYPACT and RAMS runs made for MVP Session III are presented in Table 2.

- RAMS and HYPACT data for Sessions I and II will be modeled and compiled in the next tasks for this project. Session II RAMS runs have been made.

Table 2. Listing of HYPACT and RAMS runs made for MVP Session III. The size of each directory containing the data in 1024-byte units is presented.

	HYPACT Data		ERDAS RAMS data		PROWESS RAMS data	
MVP Release Number	ERDAS size (1024-byte units)	RAMS size (1024-byte units)	Run directory (yymmddtttt)	size (1024-byte units)	Run directory (yymmdd.tt)	size (1024-byte units)
301	14996	31920	9604261200	112260	960426.12	269604
302	17460	32624	9604271200	102632	960427.12	"
303	12056	12052	9604271200	"	960427.12	404816
304	32444	33608	9604281200	123204	960428.12	261928
305	11280	14312	9604281200	"	960428.12	"
306-307	37516	48920	9604291200	107284	960429.12	254852
308	47248	122528	9605010000	112500	960501.00	353724
309	27256	64624	9605011200	110904	960501.12	233876
310	30068	62584	9605020000	110300	960502.00	353756
311	25052	35276	9605020000	"	960502.12	217500
313	32024	42500	9605031200	110304	960503.12	253476
314	13928	20072	9605031200	"	960503.12	"
315	53356	92064	9605041200	104996	960504.12	253776
316	17880	16868	9605041200	"	960504.12	"
317	17580	22140	9605051200	110272	960505.12	332276
318	24024	24764	9605051200	"	960505.12	"
319	32248	40508	9605061200	110288	960506.12	348876
320	18944	19448	9605061200	"	960506.12	"
321	70196	77820	9605090000	111112	960509.00	353780

SUBTASK 6   EXTEND 29-KM ETA MODEL OBJECTIVE EVALUATION (MR. NUTTER)

In order to increase statistical sample sizes and to evaluate the effects of ongoing eta model development, the AMU has extended the objective evaluation of meso-eta surface and upper-air point forecast accuracy. In November, Mr. Nutter completed the development of new software necessary to perform the statistical verification. Using the new software, statistics were generated for the 1996 warm season, the 1996 cool season, and the 1997 warm season. Several graphs were plotted to establish basic error characteristics and to begin seasonal comparisons of forecast accuracy. Data collection for the 1997 cool season will conclude at the end of January 1998.

In the previous AMU quarterly report (Fourth Quarter FY-97), preliminary results from the twin warm season evaluation of surface forecast accuracy were presented. Those results indicated that a statistically significant change in 2-m temperature forecast bias occurred and was likely caused by an update to the eta model's radiation parameterization. In the following sections, some early results from the analysis of upper-air forecast accuracy are presented.

Eta Model Overview

Except for differences in duration, resolution, and data assimilation, the 48-km "early" eta and 29-km "meso" eta models have been running with the same configuration since 31 January 1996. On 18 February 1997, components of the radiation, cloud, and surface moisture processes were updated in both models (EMC 1997). Then on 19 August 1997, calculation of the model's planetary boundary layer depth was adjusted. Substantial changes are planned for the early-eta in January 1998 that will include an increase in the model's horizontal and vertical resolution. Specific details regarding the dynamics, physics, horizontal domain, initialization, and other aspects of the eta model configuration are provided by Black (1994), Janjic (1994), Rogers et al. (1995, 1996), and Zhao et al. (1997).

Data

Local station or point forecasts from the 0300 UTC and 1500 UTC meso-eta model cycles are extracted from the meso-eta model grid point nearest to selected rawinsonde observation sites. Under the current configuration, meso-eta point forecasts provide hourly data for a duration of 33 hours. Rawinsonde observations are collected twice daily from Edwards Air Force Base, CA (EDW), Cape Canaveral Air Station, FL (XMR), and Tampa Bay, FL (TBW).

Analysis

The objective verification of the meso-eta model focuses on the overall accuracy of wind, temperature, and moisture forecasts at the three stations mentioned above. The statistical measures used to quantify model forecast errors are the bias (forecast – observed), root mean square (RMS) error, and error standard deviation. Using these statistics, point forecasts from the meso-eta model are verified against standard surface and upper air observations. In order to assess the significance of differences between sample means for a given parameter (e.g. seasonal changes in average temperature or wind speed), the standardized Z-statistic (Walpole and Meyers 1989) is calculated and compared with the normal distribution using a 99% confidence level ($\alpha = 0.01$). A variance inflation factor is applied during the calculation of Z in order to adjust for the influence of serial dependence, or persistence, within the seasonal time series (Wilks 1995). A more extensive discussion of the evaluation criteria is presented by Nutter and Manobianco (1997) and Manobianco and Nutter (1997).

For quality control, gross errors in the data are screened manually and corrected, if possible. Error values which are greater than three standard deviations from the mean forecast minus observed differences are excluded from the final statistics. This procedure is effective at flagging bad data points and removes less than one percent of the data. Because a good estimate of the population variance is

obtained from samples of size $n \geq 30$ (Walpole and Meyers 1989), results are disregarded if a sample of parameters at a given time or vertical level contains less than thirty members. To the nearest order of magnitude, most of the results shown here are calculated from samples containing roughly one hundred data points.

Results

The results presented in this section focus on the objective verification of upper air forecasts for temperature, mixing ratio and wind speed as function pressure at XMR, TBW, and EDW. Analysis of results presented here incorporates data from the 1996 cool season and both the 1996 and 1997 warm seasons. Verification of forecasts for surface and other upper air parameters is not discussed at this time.

Throughout each 33-h forecast period, there are typically three rawinsondes available for verification. Examination of statistics corresponding to each of these verification times (not shown) does not reveal any substantially different error characteristics. This result is consistent with those reported by Manobianco and Nutter (1997). In order to enhance the sample size, statistics for the 0300 and 1500 UTC forecast cycles were then calculated after combining all available forecast/observation pairs regardless of their verification time. Errors associated with each forecast cycle (not shown) also display similar characteristics. Given these attributes, the results discussed in the following sections represent a seasonal blend of all valid forecast/observation pairs from both the 0300 and 1500 UTC model cycles.

Since data from both the 1996 and 1997 warm seasons are available, it is desirable to consider the significance of seasonal differences in mean error characteristics. Such differences could be caused (a) by inter-annual variability in the observations, (b) by a change in forecast accuracy resulting from model updates, or (c) from some combination of these effects. Examination of standardized Z-statistics (not shown) reveals that there were no statistically significant seasonal changes in mean forecast error that could be attributed individually to seasonal changes in either the forecasts or the observations. This result is not surprising since the bundle of eta model changes implemented in February 1997 were designed primarily to affect surface forecasts (EMC 1997). Since there are no significant differences between the seasonal biases, a composite is formed from all data collected during both warm season evaluation periods to develop a general profile of meso-eta error characteristics at XMR, TBW, and EDW. At this time, only results for the 1996 cool season are available but will be updated with the 1997 cool season data during the next quarter.

Temperature

Warm season temperature biases at EDW are less than ± 1 °C (Fig. 11). At XMR and TBW, biases below 700 mb are about 1 °C colder than observed whereas above 700 mb they become nearly 2 °C warmer than observed. The net effect for warm season forecasts at the Florida stations is a tendency towards a thermally stable model atmosphere. RMS errors range from about 1 to 2.5 °C and are largest in the upper troposphere (Fig. 11b). In comparison, typical RMS uncertainty in rawinsonde temperature observations is about 0.6 °C (Hoehne 1980; Ahnert 1991) which suggests that almost half of the error in the middle troposphere may be due to measurement uncertainty.

During the cool season, temperature forecasts at EDW exhibit a cool bias below 700 mb that exceeds -4 °C near the surface (Fig. 11c). At XMR and TBW, temperature errors are less than 1 °C except near the 700 mb level and above the tropopause. Examination of forecast and observed soundings at XMR throughout the cool season (not shown) reveals that the 700 mb cold bias appears primarily because model forecasts of the lower tropospheric inversion are frequently higher than actually observed. RMS errors in temperature forecasts are largest at EDW with values ranging from about 2 to 3 °C except near the surface (Fig. 11d). Since biases are small, this result suggests there is a substantial amount of daily variability in either the forecasts or observations.

Mixing Ratio

Warm season mixing ratio biases at XMR and TBW (Fig. 12a) indicate that meso-eta forecasts are about 1 g kg^{-1} too dry below 700 mb. Conversely, biases above 500 mb suggest that forecasts at these locations tend to retain larger amounts of moisture than observed. In combination with the cool lower tropospheric temperature biases discussed in the previous section, these results suggest that warm season model forecasts at XMR and TBW are typically more stable than observed. At EDW, mixing ratio biases below 700 mb are about 0.5 g kg^{-1}. During the cool season, mixing ratio biases at all three stations are slightly wet or near zero at most levels (Fig. 12c) except for the dry layer which appears between 950 and 800 mb at XMR and TBW.

RMS errors for both warm and cool seasons (Figs. 13b, d) drop from around 2 g kg^{-1} at low-levels (1.5 g kg^{-1} at EDW) to near zero at 200 mb, where there is very little water vapor present in the atmosphere. Results shown in Figs. 13b, d are consistent with those of Rogers et. al (1996), who show 24-h RMS errors in specific humidity from 48-km eta model forecasts across the United States during September 1994 ranging from nearly 2 g kg^{-1} at 1000 mb to less than 0.1 g kg^{-1} at 250 mb (see their Fig. 7). Note that these calculations for mixing ratio errors are not normalized by magnitude and are therefore not representative of percent errors as the mixing ratio tends toward zero in the upper troposphere.

Wind Speed

Warm season wind speed biases are generally less than ±1 m s^{-1} (Fig. 13a). The exception occurs at EDW where lower tropospheric wind speed forecasts are about 2 m s^{-1} slower than observed. This result is consistent with a slowness in 10-m wind speed forecasts identified at EDW by Manobianco and Nutter (1997). Below 400 mb, warm season RMS errors range from about 2 to 4 m s^{-1} (Fig. 13b). RMS errors around the 200 mb level are larger with values approaching 6 m s^{-1}. Since forecast biases are small and uncertainties in rawinsonde wind speed measurements are about 3.1 m s^{-1} (Hoehne 1980), much of the total RMS wind speed error especially at lower levels could result from observational uncertainty.

During the cool season, forecast wind speeds at XMR and TBW are about 1 m s^{-1} slower (faster) than observed in the middle (upper) troposphere (Fig. 13c). At EDW, wind speed biases exhibit sharp variations with height but remain generally within ±2 m s^{-1} except near the surface. Cool season RMS errors at XMR and TBW are comparable to those found during the warm season and as above, likely receive large contributions from observational measurement uncertainties (Fig. 13d). RMS errors at EDW are substantially larger with some values exceeding 10 m s^{-1}.

Temperature Errors (^{o}C)
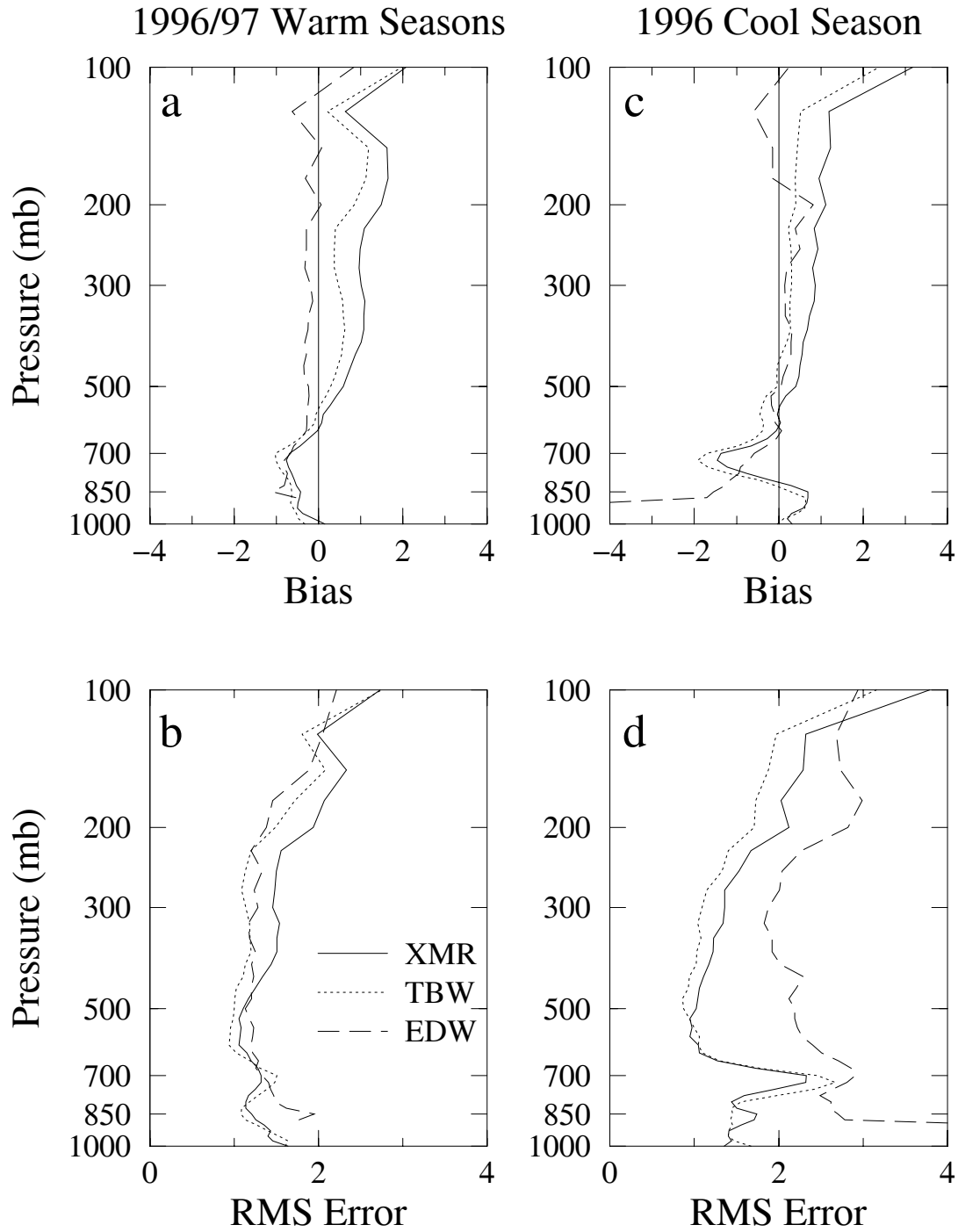
Figure 11.   Bias and RMS error profiles for meso-eta temperature forecasts (°C) at XMR (solid lines), TBW (dotted lines), and EDW (long dashed lines). Panels a and b show May through August 1996 and 1997 bias and RMS errors plotted as a function of pressure. Panels c and d show bias and RMS errors from October 1996 through January 1997.

Mixing Ratio Errors (g kg⁻¹)
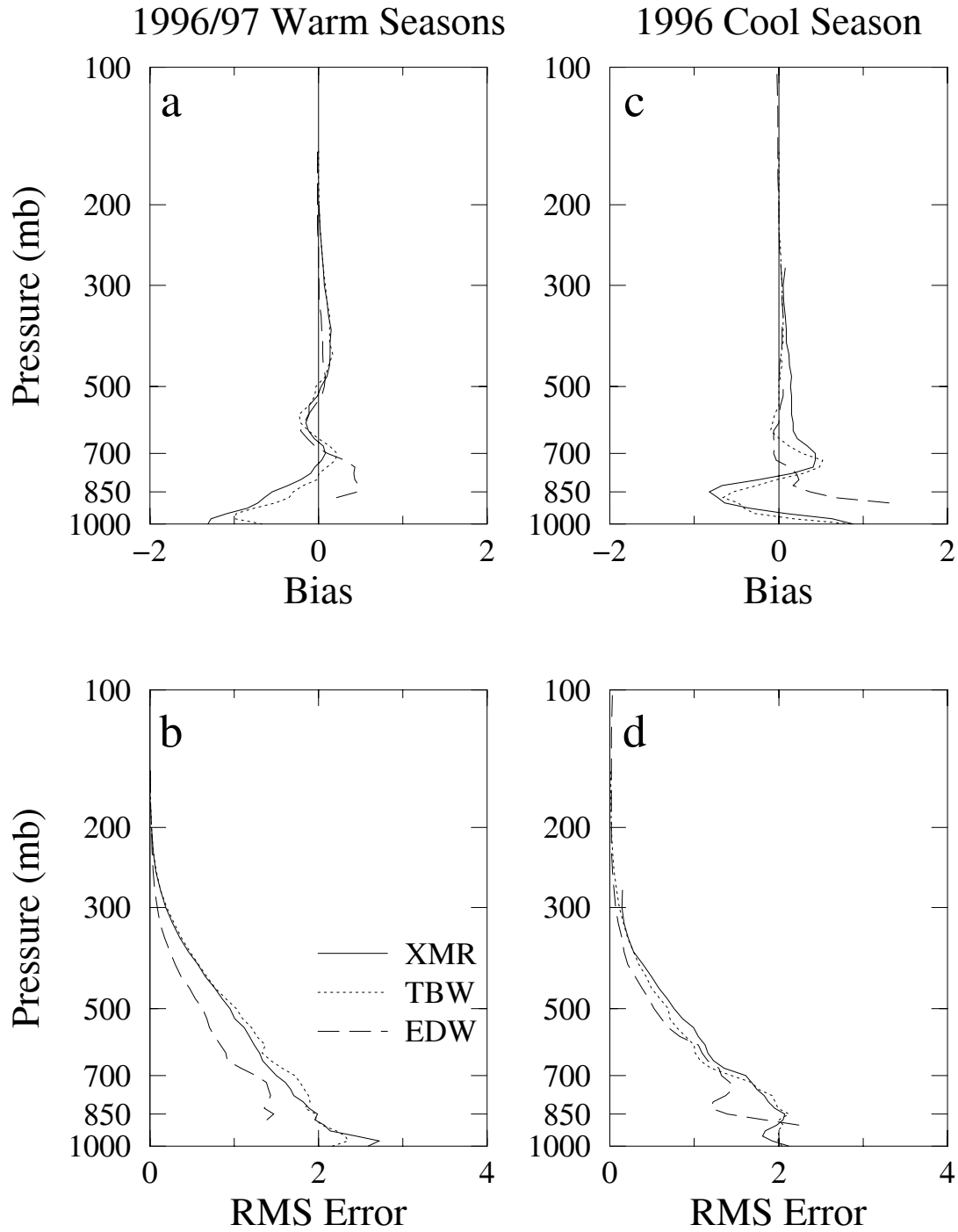
Figure 12. Bias and RMS error profiles for meso-eta mixing ratio forecasts (g kg⁻¹) at XMR (solid lines), TBW (dotted lines), and EDW (long dashed lines). Panels a and b show May through August 1996 and 1997 bias and RMS errors plotted as a function of pressure. Panels c and d show bias and RMS errors from October 1996 through January 1997.

Wind Speed Errors (m s^{-1})

1996/97 Warm Seasons

1996 Cool Season
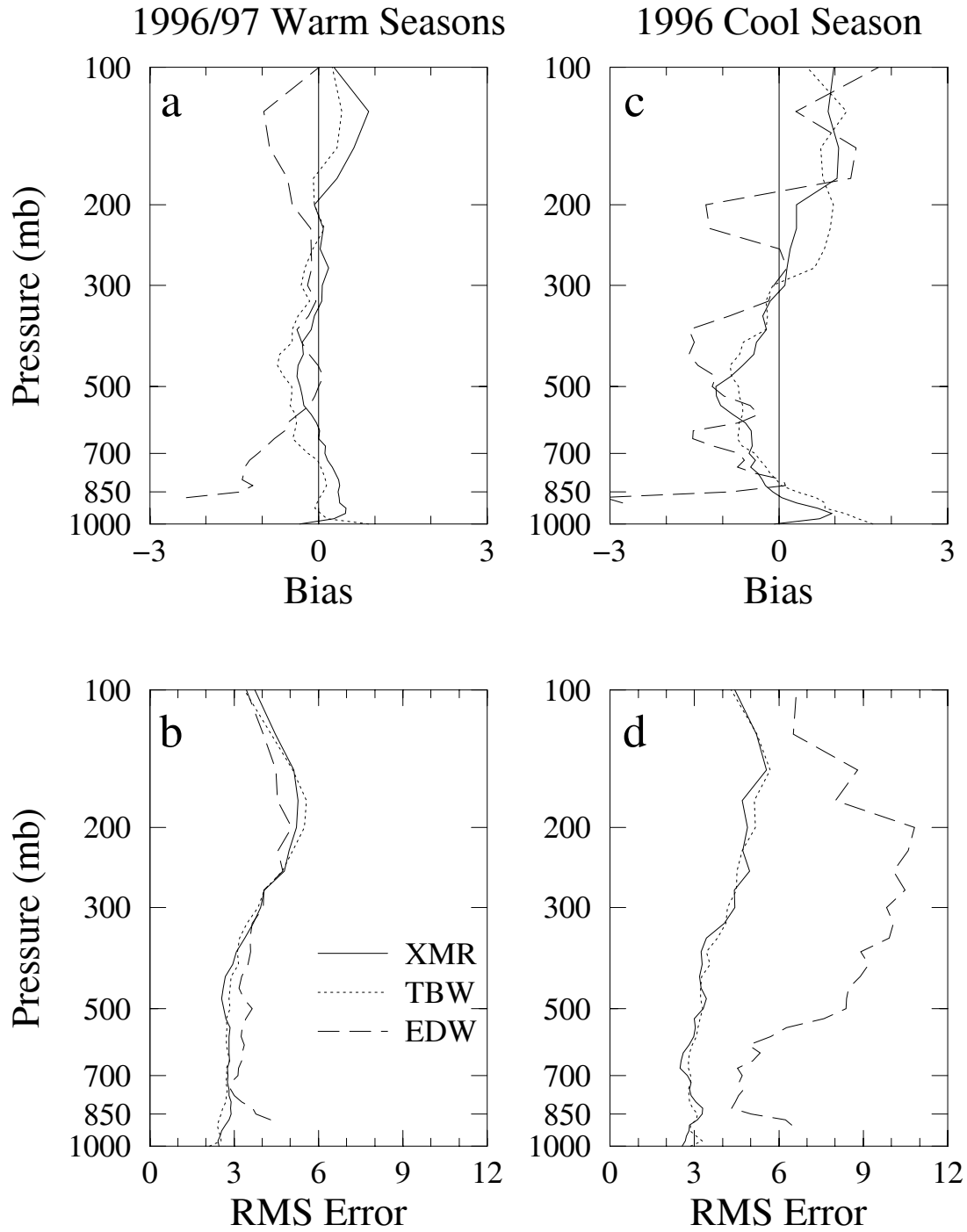
Figure 13.   Bias and RMS error profiles for meso-eta wind speed forecasts (m s^{-1}) at XMR (solid lines), TBW (dotted lines), and EDW (long dashed lines). Panels a and b show May through August 1996 and 1997 bias and RMS errors plotted as a function of pressure. Panels c and d show bias and RMS errors from October 1996 through January 1997.

References

Ahnert, P. R., 1991: Precision and compatibility of National Weather Service upper air measurements. Preprints, *Seventh Symp. on Meteorological Observations and Instrumentation*, New Orleans, LA, Amer. Meteor. Soc., 221-226.

Black, T. L., 1994: The new NMC mesoscale eta model: description and forecast examples. *Wea. Forecasting*, 9, 265-278.

EMC, cited 1997: Environmental Modeling Center: Mesoscale Modeling Branch FAQ. [Available on-line from http://nic.fb4.noaa.gov:8000/research/FAQ-eta.html.]

Hoehne, W. E., 1980: *Precision of National Weather Service Upper Air Measurements*. NOAA Tech. Memo. NWS T&ED-16.

Janjic, A. I., 1994: The step-mountain Eta coordinate model: Further developments of the convection, viscous sublayer, and turbulence closure schemes. *Mon. Wea. Rev.*, **122**, 927-945.

Manobianco, J. M., and P. A. Nutter, 1997: Evaluation of the 29-km Eta Model for Weather Support to the United States Space Program. NASA Contractor Report CR-205409, Kennedy Space Center, FL, 103 pp. [Available from ENSCO, Inc., 1980 N. Atlantic Ave., Suite 230, Cocoa Beach, FL 32931].

Mesinger, F., 1996: Improvements in quantitative precipitation forecasts with the eta regional model at the National Centers for Environmental Prediction: The 48-km upgrade. *Bull. Amer. Meteor. Soc.*, 11, 2637-2649.

Nutter, P. A., and J. M. Manobianco, 1997: Evaluating the potential utility of the meso-eta model for weather support to the US space program. Preprints, *7th Conference on Aviation, Range and Aerospace Meteorology*, Long Beach, CA, Amer. Meteor. Soc., 420-425.

Rogers, E., D. G. Deaven, and G. J. DiMego, 1995: The regional analysis system for the operational "early" eta model: Original 80-km configuration and recent changes. *Wea. Forecasting*, **10**, 810-825.

Rodgers, E., T. L. Black, D. G. Deaven, G. J. DiMego, Q. Zhao, M. Baldwin, N. Junker, and Y. Lin, 1996: Changes to the operational "early" eta analysis/forecast system at the National Centers for Environmental Prediction. *Wea. Forecasting*, 11, 391-413.

Walpole, R. E., and R. H. Meyers, 1989: Probability and Statistics for Engineers and Scientists. Macmillan, Inc., New York, 765 pp.

Wilks, D. S., 1995: *Statistical Methods in the Atmospheric Sciences*. Academic Press, Inc., San Diego, CA, 467 pp.

Zhao, Q., T. L. Black and M. E. Baldwin, 1997: Implementation of the cloud prediction scheme in the Eta model at NCEP. *Wea. Forecasting*, 12, 697-712.

SUBTASK 7   DATA ASSIMILATION MODEL / CENTRAL FLORIDA DATA DEFICIENCY (DR. MANOBIANCO)

The data assimilation model / central Florida data deficiency task has three main components.

- Identify all existing meteorological data sources (government, agricultural, utility, etc.) that lie within 160 km of KSC/CCAS,

- Identify an appropriate data assimilation model that incorporates and analyses all existing central Florida meteorological data sources in a dynamically consistent manner, and

- Implement a working prototype of the data integration model and perform a proof-of-concept test through post-analysis of selected weather events for two days.

During the past quarter, Dr. Manobianco and Mr. Nutter completed data collection for a central Florida warm season case study, installed and configured a Local Data Integration System (LDIS), and began investigating the utility provided by a post-analysis of the warm season weather event. The following sections highlight AMU progress on the task during the past quarter.

Data Collection

The availability, frequency, and density of local data sources across central Florida were documented in the previous AMU quarterly report (Fourth Quarter FY-97). During the past quarter, Dr. Manobianco assembled a complete collection of these data from 26-27 July 1997 for a warm season case study using the local data integration model. This case is interesting because an outflow boundary from thunderstorms to the southwest of KSC/CCAS produced winds in excess of 30 kt shortly after the MST was removed during an Atlas launch count. As a result of the strong winds, the MST was returned and the launch was scrubbed for the day.

Because all data sets for this case were not archived by any single group, Dr. Manobianco retrieved data from several different sources. The background RUC fields were obtained from the Atmospheric Radiation Measurement program external data center archive. The surface METAR observations were provided by Dr. Kenneth Waight at MESO, Inc. The KSC/CCAS mesonet tower and KSC 50 MHz profiler data were restored from 9-track tape to MIDDS by CSR personnel. The 915 MHz profiler data were restored from 8-mm tape to the AMU UNIX workstations by Ms. Winnie Lambert. The level II NEXRAD data were provided on 8-mm tape by NWS MLB. The GOES-8 soundings were provided by Mr. Timothy Schmit from NOAA NESDIS (Madison, WI). The GOES-8 cloud-track and water vapor winds were provided by Mr. Chris Veldon from the Cooperative Institute for Meteorological Satellite Studies (Madison, WI). Lastly, aircraft data (PIREP and ACARS) were provided by Mr. Matt Nitta from the Forecast Systems Laboratory.

Mr. Nutter began data collection from 11-12 December 1997 for a cool season case study. The presence of a stationary front across central Florida on these days created a challenging forecast situation that included heavy rain and strong gusty winds with imbedded thunderstorms. Examination of surface observations and 915 MHz profiler data in real time clearly indicated the frontal passage across KSC/CCAS between 1000 and 1100 UTC. Later, as the front slowly approached the MLB NEXRAD site, it became visible on radar as a line of enhanced reflectivity and a well-defined wind shift.

LDIS Configuration

There are currently two data integration systems being considered as candidates for the LDIS. These include the ARPS (Advanced Regional Prediction System) Data Assimilation System (ADAS; Brewster 1996) and the Local Analysis and Prediction System (LAPS; McGinley 1995). ADAS/ARPS is available from the Center for Analysis and Prediction of Storms (CAPS) at the University of Oklahoma (Norman, OK) and LAPS is available from NOAA's Forecast Systems Laboratory (FSL; Boulder, CO).

In November, an upgraded version of the LAPS software was acquired, configured for local implementation over central Florida, and installed on the AMU's IBM workstation. However, the LAPS software is not well documented and contains directory structures and file formats that are difficult to implement on local computers. Therefore, initial efforts have focused on the installation and

25

configuration of ADAS for use as a LDIS. However, since the current version of ADAS is unable to ingest satellite data, the AMU will continue to consider both LAPS and ADAS until it becomes clear which of these software systems are most appropriate for use in east-central Florida.

The preliminary configuration for the LDIS using ADAS contains outer and inner grids with horizontal resolutions of 10 and 2 km, respectively and 40 vertical levels. The 10-km (2-km) analysis domain is centered over Cape Canaveral, Florida and covers 400 x 400 km (160 x 160 km). The RUC is used as a first guess for analyses of observational data on the 10-km domain. Currently, NCEP generates three-dimensional RUC analyses every 3 hours at a horizontal resolution of 60 km with 25 vertical levels. Between the 3-h RUC updates, new 10-km analyses are generated every 15 minutes using observational data and a background field from the previous 10-km analysis cycle (Fig. 14). The resulting 10-km products are then used as background fields to analyze observational data at 15-min intervals on the 2-km domain (Fig. 14).

The analyses in ADAS are produced following Bratseth (1986) who developed an iterative successive correction method which converges to statistical or optimum interpolation (OI). The Bratseth scheme is more computationally efficient than OI but has the advantages of OI schemes which account for variations in data density and errors in the background fields and observations. The analyses on both the 10-km and 2-km grids are produced using three passes of the Bratseth scheme with successively smaller correlation distances and radii of influence. With such an approach, it is possible to control how closely the scheme fits the data and the wavelength of features present in the final analysis.

As work on this task proceeds, the current LDIS configuration will likely be adjusted to improve the analysis products. For example, the relative weights assigned to observational data during the analysis cycles may be revised. Also, the configuration shown in Fig. 14 does not yet address temporal discontinuities in the analyses which may result when new RUC background fields are updated at 3-h intervals. Cycling the 2-km analyses with observation updates every 5 minutes could provide greater temporal continuity for time animations as proposed by the light gray squares in Fig. 14. Finally, it may be desirable to use prognostic fields from either a local mesoscale model or the RUC as a background for analyses on the 10-km and/or 2-km grids.

Preliminary Case Study Results

A warm season case event has been selected from 26-27 July 1997 to investigate the capabilities and utility provided by LDIS analyses. The case was characterized by a typical, undisturbed warm season environment. Early in the afternoon, scattered thunderstorms developed across the peninsula (Fig. 15a) and a sea-breeze was evident along the east coast. Later in the afternoon, strong thunderstorms developed to the southwest of KSC/CCAS and were evident on both radar (not shown) and GOES-8 satellite imagery (Fig. 15b). An outflow boundary from these storms propagated to the northeast and caused an increase in wind speeds that was noted on KSC/CCAS mesonet towers around 2245 UTC. This outflow boundary forced Atlas launch operation A1393 to be scrubbed for the day.

Dr. Manobianco completed the minimal configuration and data reformatting necessary to run ADAS on this 26-27 July 1997 case. Both 10-km and 2-km grid analyses were run at 15-min intervals (e.g. Fig. 14) from 2100 UTC 26 to 0000 UTC 27 July using only surface METAR, KSC/CCAS mesonet, and level II NEXRAD data. The resulting analyses discussed below show the fine-scale evolution of the outflow boundary. Future work will incorporate all available data collected for this case, possibly using different LDIS configurations.

A plot of 10-m potential temperature from the 10-km analysis at 2100 UTC (Fig. 16a) indicates that a temperature gradient exists across central Florida. Temperatures over the southwestern part of the domain are about nine degrees warmer than those to the northeast. Maximum winds in the southeastern part of the domain are from the southeast at approximately 5 m s^{-1} (speeds not indicated). A line of

convergence in the 10-m winds appears to extend southward from near KSC/CCAS to near Lake Okeechobee. These features generally persist through later analyses and illustrate the resolution of the analyses on the 10-km grid at the 10-m height level.

Analyses are generated every 15 min (e.g. Fig. 14) but are only shown here at 30-min intervals. Even at these 30-min increments, changes in the analyses between 2100 and 2230 UTC (Figs. 17a-d) are quite subtle. The only observations influencing the analyses at this level were the KSC/CCAS mesonet data on each iteration and the statewide METAR sites at 2100 and 2200 UTC. Radar data do not affect analyses at this level because they are well above 10-m throughout the domain.
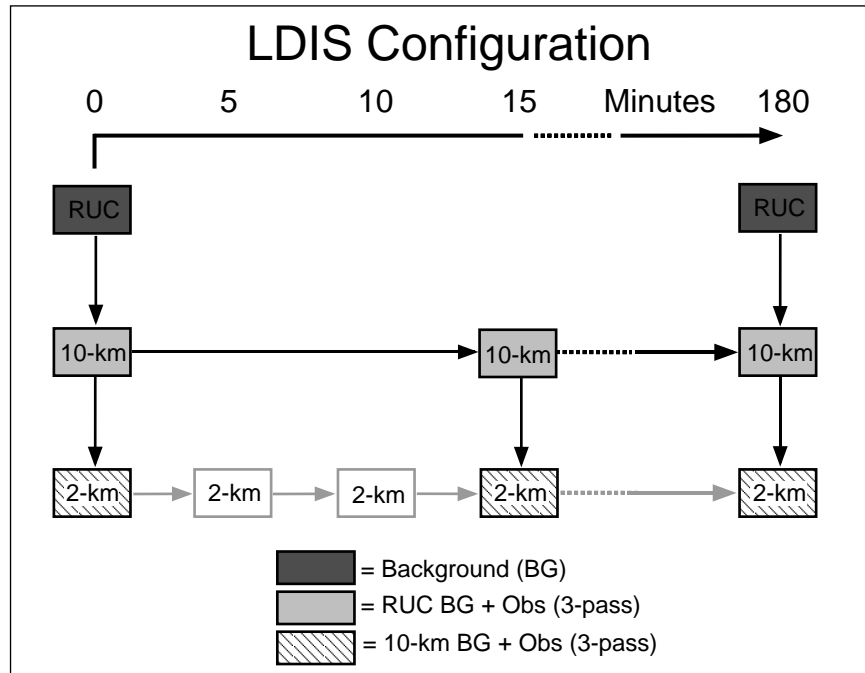
Figure 14.   Schematic diagram illustrating the preliminary LDIS configuration. See text for details.
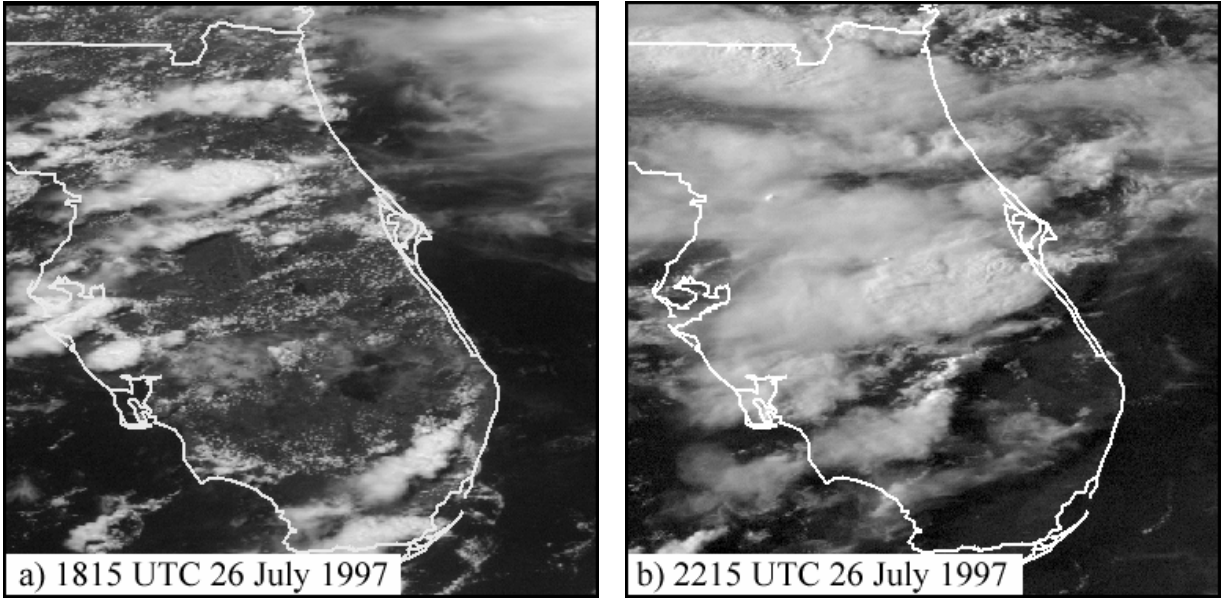
Figure 15.   GOES-8 visible satellite imagery valid (a) at 1815 UTC and (b) 2215 UTC 26 July 1997.

At 2300 UTC changes begin to occur as a substantial wind shift and decrease in temperature are noted near the center of the domain around KSC/CCAS (Fig. 16e). In addition, temperatures over the southwestern part of the domain respond to updated METAR observations and drop by about one degree. At 2330 UTC temperatures around KSC/CCAS decrease by another degree (Fig. 16f). This pool of colder air developing near the center of the domain is consistent with the passage of the thunderstorm outflow boundary observed at KSC/CCAS around 2245 UTC. It is interesting to note that although the 10-m level analyses show the developing cold pool after the passage of the outflow boundary, there are no sharp wind shifts or thermal gradients at 10-m that clearly depict the position and/or movement of the boundary on the 10-km analysis grid.

Although not clearly evident on the 10-km domain, additional details regarding the structure and evolution of the outflow boundary are found in analyses performed on the 2-km domain. High density wind vectors from the 2-km analyses are shown at the 470-m height level in Fig. 17. Analyses are plotted every 15 min and depict much greater structure to the wind field in an area to the southwest of KSC/CCAS. Between 2130 and 2145 UTC, winds in the southwestern part of the domain shift from south-southeast to southwest (Figs. 18a, b). In subsequent plots, the westerly component of the winds across the southern half of the domain intensifies until a well defined, curved deformation boundary develops around 2230 UTC (Fig. 17e) and begins to expand to the north and east (Fig. 17f). Maximum wind speeds near the leading edge of the boundary (not indicated) are about 12-14 m s^{-1}. As discussed below, the outflow boundary is most strongly depicted on the 2-km domain near the 470-m level.

Above the lowest 2 to 3 height levels, surface data do not influence the analyses. Changes in the horizontal wind field above the surface therefore develop in response to NEXRAD radial velocities in areas where radar reflectivity targets are available. Examination of level II radar reflectivity and radial velocity data (not shown) indicates that features present in the high resolution wind analyses (Fig. 17) are consistent with the scale and motion of patterns associated with the observed thunderstorm. It should be noted that the detailed structure of horizontal winds associated with this boundary would likely be more difficult to visualize in real-time using only radial velocity displays.

Cross sections taken along SW-NE oriented lines drawn in Fig. 17 help to illustrate the vertical structure and evolution of wind speeds analyzed on the 2-km domain. At 2145 UTC a small wind speed maximum first appears at a height of 500 m near the left side of the figure (Fig. 18b). During the next 30

minutes, this wind speed maximum intensifies through a deeper layer while propagating slowly to the northeast (Figs. 18b-d). At 2230 UTC a core of strong winds near the 500-m level separates and moves ahead of the larger core of winds above it (Fig. 18e). Fifteen minutes later, two distinct cores of strong horizontal winds become well organized with wind speeds in excess of 10 m s^{-1} (Fig. 18f).

As discussed above, updates to the horizontal wind analysis above the surface are derived solely from NEXRAD radial winds in areas where reflectivity targets are available. Independent examination of NEXRAD reflectivity data (not shown) indicate that the 2- to 3-km wind speed maxima that appear in the LDIS analyses (Figs. 18d-f) are associated with an area of heavy rain moving from southwest to northeast. Consistent with this storm motion, wind directions in the analyses between 2 and 3 km are also from the southwest (directions not indicated). However, it will be necessary to subtract storm motion from the total horizontal winds depicted in Fig. 18 in order to determine what fraction forms solely in response to storm-relative winds.
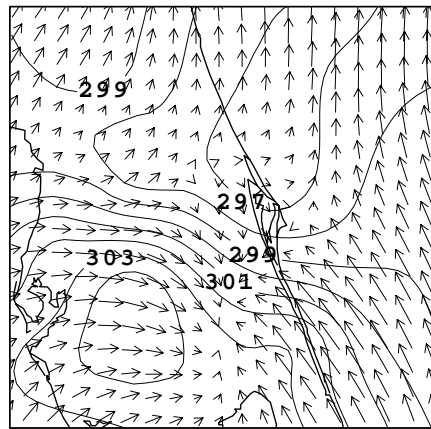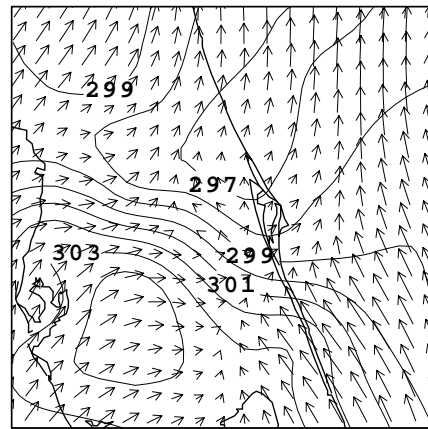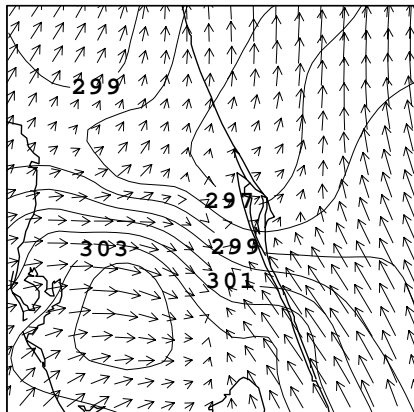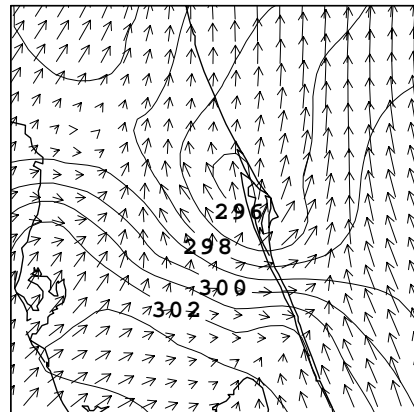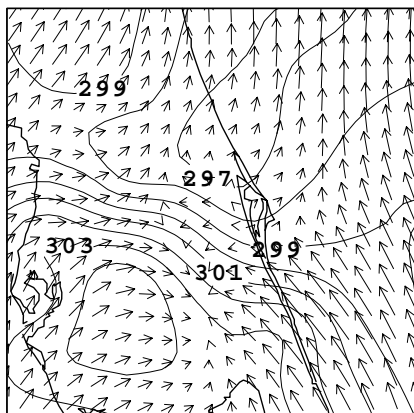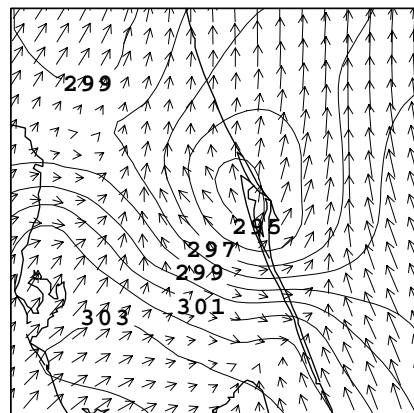
Figure 16.   Wind vectors (m s⁻¹) and isotherms of 10-m potential temperature (K) at 10-m across the 10-km analysis domain. Analyses are shown every 30 min from (a) 2100 UTC through (f) 2330 UTC 26 July 1997.
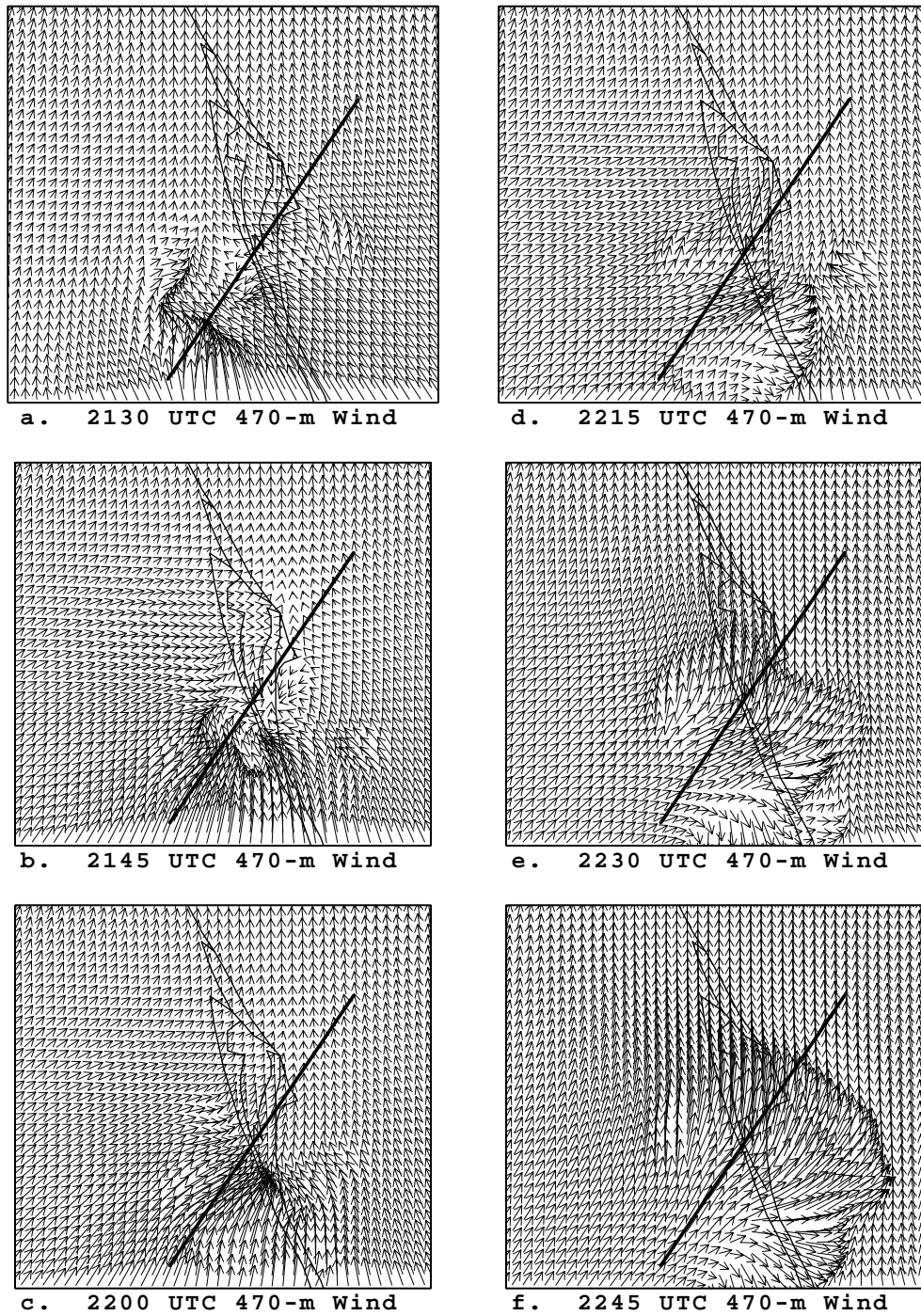
Figure 17.   Wind vectors on the 2-km analysis domain at the 470-m height level. Plots are shown
every 15 min from (a) 2130 UTC through (f) 2245 UTC 26 July 1997. The heavy solid lines
denote the locations of the SW-NE oriented cross-sections shown in Fig. 18.

31
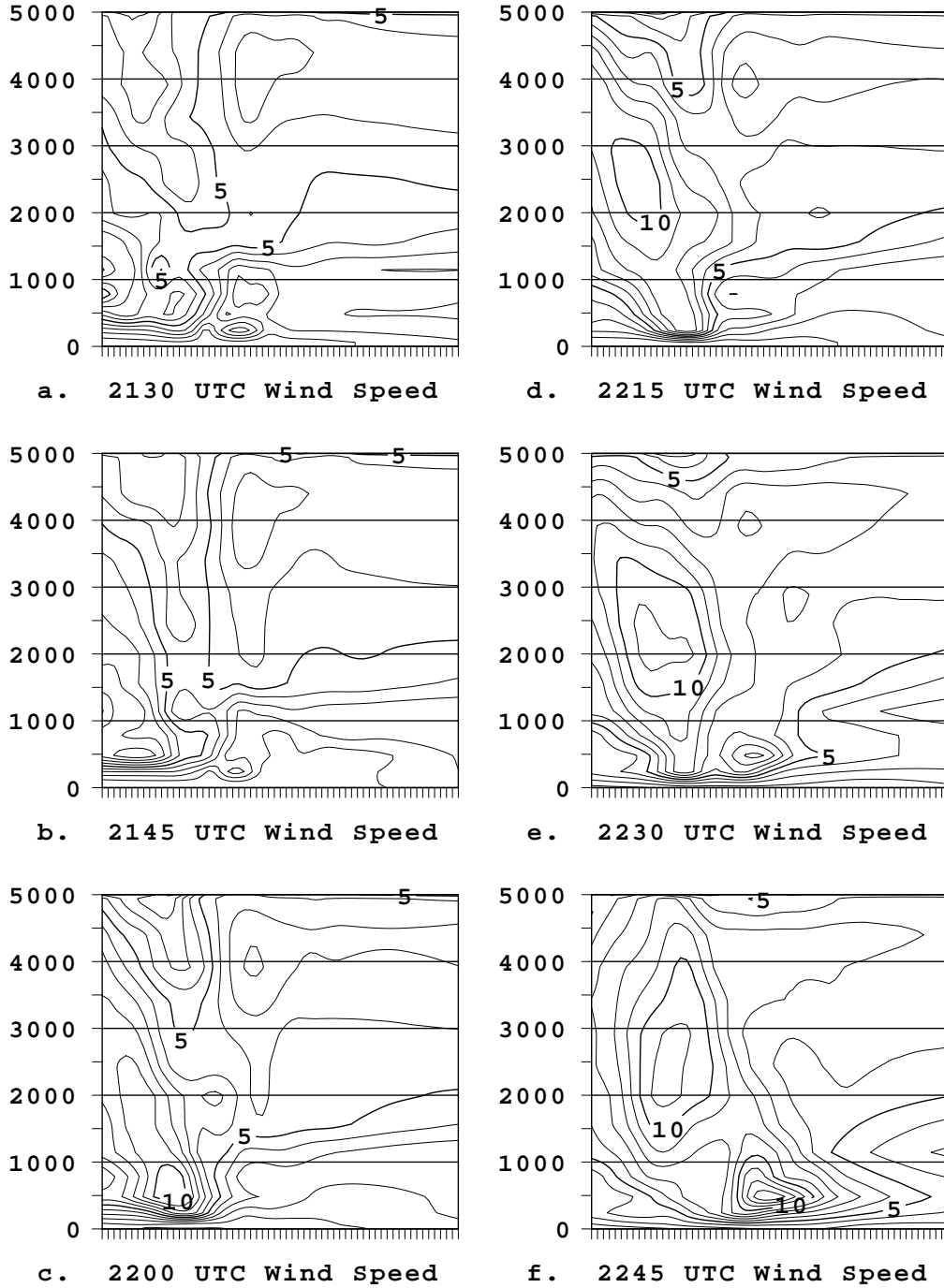
Figure 18.   Cross-section plots of wind speed (m s^{-1}) as a function of height (m) along the SW-NE (left-to-right) oriented lines from the 2-km analysis domain shown in Fig. 17. Isotachs are plotted at 1 m s^{-1} intervals with emphasis every 5 m s^{-1}. Plots are shown every 15 min from (a) 2130 UTC through (f) 2245 UTC 26 July 1997.

At the 500-m level, the separate core of maximum winds moving ahead of the mid-level feature is indicative of the storm's outflow boundary. Since NEXRAD radial velocities are bounded by the lowest scan elevation, the strongest wind speeds may actually occur below the 500-m level. However, inspection of KSC/CCAS wind tower data from the surface to 150 m (not shown) indicates that wind speeds do not exceed those shown in Fig. 18f. Nevertheless, it is possible that maximum wind speeds occur above 150 m and below 500 m. Although not used in these preliminary analyses, the KSC/CCAS 915 MHz boundary layer profilers can provide wind data in the layers from 150 - 500 m. Unfortunately, wind profiles from the False Cape and Titusville-Cocoa (Ti-Co) sites are contaminated by rain after 2200 UTC 26 July and therefore cannot be used to track the outflow boundary for this case.

Summary / Future Work

The foregoing sections describe the AMU's progress on the data assimilation model / central Florida data deficiency task during the past quarter. Using ADAS, a Local Data Integration System (LDIS) was minimally configured to test its analysis capabilities on a warm season case from 26-27 July 1997. Although all available data were assembled for this case, the analyses presented above utilize only a single RUC background, surface observations, and NEXRAD radial velocity data. Results from the 26-27 July case reveal that subsequent 15-min analyses of horizontal winds on the 2-km inner domain are capable of depicting the formation and propagation of a thunderstorm outflow boundary. Future analysis efforts will incorporate all available data sources while optimizing the LDIS configuration to enhance diagnostics, visualizations, and time animations.

References

Brewster, K., 1996: Application of a Bratseth analysis scheme including Doppler radar data. Preprints, *15th Conf. on Weather Analysis and Forecasting*, Norfolk, VA, Amer. Meteor. Soc., 92-95.

Bratseth, A. M., 1986: Statistical interpolation by means of successive corrections. *Tellus*, **38A**, 439-447.

McGinley, J. A., 1995: Opportunities for high resolution data analysis, prediction, and product dissemination within the local weather office. Preprints, *14th Conf. on Weather Analysis and Forecasting*, Dallas, TX, Amer. Meteor. Soc., 478-485.

2.4 *AMU CHIEF'S TECHNICAL ACTIVITIES (DR. MERCERET)*

During the past quarter, Dr. Merceret continued to advise John Lane, a Ph.D. candidate at the University of Central Florida, on a study of raindrop size distributions and their effect Z-R relations. The work is directed at improving the use of WSR-88D and rain gauge data as ground truth for NASA's TRMM project, and will serve as Mr. Lane's doctoral dissertation. It should also prove useful in using gauges to adjust or verify radar-derived rain rates, and may lead to improved NEXRAD rain rate algorithms.

In November, John Lane and Dr. Merceret met with Paul Willis at the Hurricane Research Division of NOAA/ERL in Miami to discuss the work. Mr. Willis is an internationally recognized expert in tropical cloud physics.

Dr. Merceret has been consulting with Mr. Lane and Rick Chapman of the Applied Physics Laboratory (APL) of the Johns Hopkins University (JHU) on the calibration of the JHU/APL disdrometer, which will be used for TRMM ground validation.

NOTICE

Mention of a copyrighted, trademarked, or proprietary product, service, or document does not constitute endorsement thereof by the author, ENSCO, Inc., the AMU, the National Aeronautics and Space Administration, or the United States Government. Any such mention is solely for the purpose of fully informing the reader of the resources used to conduct the work reported herein.

Acronyms

45 MXS	45th Maintenance Squadron
45 WS	45th Weather Squadron
AAD	Area-averaged Divergence
ACARS	Aeronautical Radio, Inc. (ARINC) Communications, Addressing & Reporting System
ADAS	ARPS Data Assimilation System
AFIT	Air Force Institute of Technology
AGL	Above Ground Level
AMU	Applied Meteorology Unit
APL	Applied Physics Laboratory
ARPS	Advanced Regional Prediction System
CAPS	Center for Analysis and Prediction of Storms
CCAS	Cape Canaveral Air Station
CITM	Cooperative Institute for Tropical Meteorology
CSI	Conditional Symmetric Instability
CSR	Computer Science Raytheon
DRWP	Doppler Radar Wind Profiler
EDW	Edwards Air Force Base Rawinsonde Station Identification
ERDAS	Emergency Response Dose Assessment System
FAR	False Alarm Rate
FSL	Forecast Systems Laboratory
FSU	Florida State University
FY	Fiscal Year
GPS	Global Positioning Satellite
GVAR	GOES Variable
HP	Hewlett Packard
HSS	Heidke Skill Score
HYPACT	Hybrid Particle And Concentration Transport
I&M	Improvement and Modernization
JSC	Johnson Space Center
KSC	Kennedy Space Center
LAPS	Local Analysis and Prediction System
LDIS	Local Data Integration System
MDPI	Microburst Day Potential Index
MSFC	Marshall Space Flight Center
MVP	Model Validation Program
NASA	National Aeronautics and Space Administration
NCAR	National Center for Atmospheric Research
NCEP	National Center for Environment Prediction
NEXRAD	NEXt-generation RADar
NWS MLB	National Weather Service Melbourne
PROWESS	Parallelized RAMS Operational Weather Simulation System

PIREP   Pilot Report
POD   Probability Of Detection
QC   Quality Control
RAMS   Regional Atmospheric Modeling System
RASS   Radio Acoustic Sounding Systems
REEDM   Rocket Exhaust Effluent Diffusion Model
RMS   Root Mean Square
ROCC   Range Operations Control Center
RSA   Range Standardization and Automation
RUC   Rapid Update Cycle
RWO   Range Weather Operations
SCIT   Storm Cell Identification and Tracking
SMG   Spaceflight Meteorology Group
SNR   Signal to Noise Ratio
USAF   United States Air Force
TBW   Tampa Bay area Rawinsonde Station Identification
Ti-Co   Titusville-Cocoa
TRMM   Tropical Rainfall Measuring Mission
VIL   Vertically Integrated Liquid
WATADS   WSR-88D Algorithm Testing And Display System
WRP   Weather Research Program
WSR-88D   Weather Surveillance Radar - 88 Doppler
XMR   Cape Canaveral Rawinsonde Station Identification

Appendix A

AMU Projects	Milestones	Target Begin Date	Target Completion Date (TCD)	Notes/Status
Cell Trend Comparison of WATADS vs. WSR-88D	Evaluate Effectiveness/Utility of 88D Cell Trends	Apr 97	Sep 97	Completed
	Final Report	Oct 97	Jan 98	2-Week Delay
Boundary Layer Profilers	Task Work Plan	Apr 97	Jun 97	Completed
	Data Collection	May 97	Aug 97	Completed
	Cool Season Data Collection	Nov 97	Mar 98	Ongoing
	Wind Data Quality Objective	May 97	Jan 98	On schedule
	Interim Report	Jan 98	Feb 98	On schedule
	RASS Data Quality Objective	Feb 98	Apr 98	On schedule
	Final Report	Apr 98	May 98	On schedule
AF I&M and RSA Support	Review Document / Products, Attend Meetings / Reviews, Document Advice, Suggestions, and Comments	Jul 96	Ongoing	On schedule
Data Integration Model / Data Deficiency	Identify Mesoscale Data Sources in central Florida	May 97	May 98	On schedule
	Identify / Install Prototype Analysis System	Aug 97	Apr 98	On Schedule
	Case Studies Including Data Non-incorporation	Nov 97	Apr 98	On schedule
	Final Report	May 98	Jul 98	On schedule
29-km Eta Model Evaluation Extension	Archive data for 1997/1998	May 97	Jan 98	On schedule
	Perform Analysis	Sep 97	Feb 98	On schedule
	Final Report	Mar 98	Apr 98	On schedule
GVAR Sounder Products Evaluation	Final Report	Apr 98	Dec 98	On schedule

The title rows of the table read: "AMU Project Schedule / 31 January 1998"

AMU Project Schedule 31 January 1998				
AMU Projects	Milestones	Target Begin Date	Target Completion Date (TCD)	Notes/Status
Delta Explosion Analysis	Analyze Radar Imagery	June 97	Nov 97	Completed
	Run Models/ Analyze Results	June 97	Feb 98	Delayed 2 months- effort has been on MVP
	Final Report	Feb 98	Mar 98	same as above
Model Validation Program	Inventory and Conduct RAMS runs for Sessions I, II, and III	July 97	Mar 98	Session III completed
	Run HYPACT for all MVP releases	Aug 97	Mar 98	Session III PROWESS completed
	Deliver data to NOAA/ATDD	Oct 97	Mar 98	On Schedule
	Acquire met data for Titan launches	July 97	Mar 98	On Schedule